(12) UK Patent Application (19) GB (11) 2 336 472 (13) A

(43) Date of A Publication 20.10.1999

(21) Application No 9213786.8

(22) Date of Filing 22.06.1992

(30) Priority Data
(31) 9115970 (32) 24.07.1991 (33) GB

(51) INT CL[6]
H01Q 17/00

(52) UK CL (Edition Q)
H1Q QEJ

(56) Documents Cited
EP 0015804 A US 3887920 A

(58) Field of Search
UK CL (Edition K) H1Q QEC QEJ QEX QKJ
INT CL[6] H01Q 1/42 15/00 15/14 17/00

(71) Applicant(s)
The Secretary of State for Defence
(Incorporated in the United Kingdom)
Defence Evaluation and Research Agency, Ively Road,
FARNBOROUGH, Hants, GU14 6TD, United Kingdom

(72) Inventor(s)
Andrew James Mackay
Michael Adrian Wood

(74) Agent and/or Address for Service
D/IPD DERA Formalities
A4 Building, Ively Road, FARNBOROUGH, Hants,
GU14 0LX, United Kingdom

(54) Abstract Title
Frequency selective absorbent structure

(57) The structure 10 has a layered construction. It includes a conducting layer 12, a central layer 14 of thickness h and a patterned conducting layer 16 of thickness g, these layers being successively disposed. The patterned layer 16 has an array of slots such as 18. In the central layer 14, the product of propagation loss/unit length and thickness h lies in the range 0.005 to 0.1. The structure is able to absorb incident energy by means of the excitation of surface waves in the substrate layer 14. This enables the dielectric layer to be thin.

Fig. 1(a).

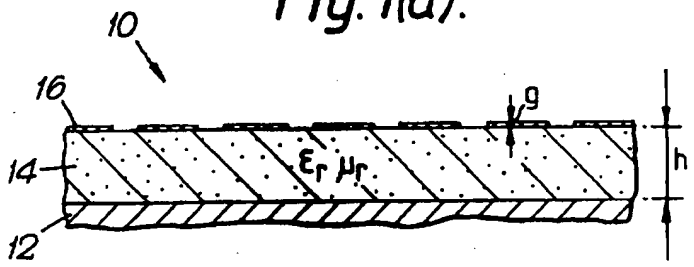

Fig. 1(b).

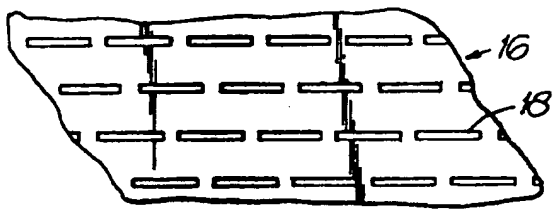

GB 2 336 472 A

Fig. 1(a).

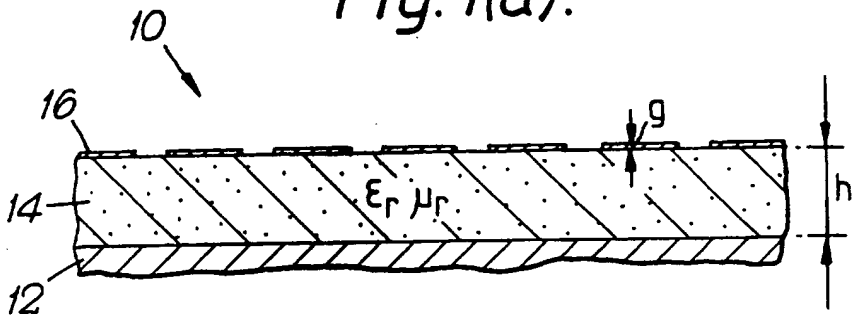

Fig. 1(b).

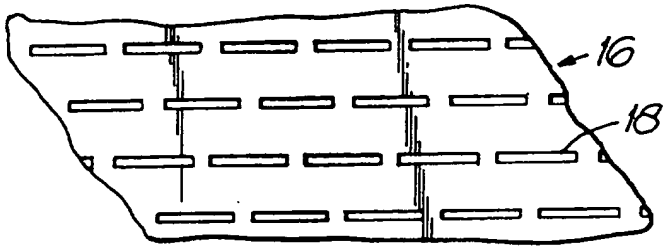

Fig. 1(c).

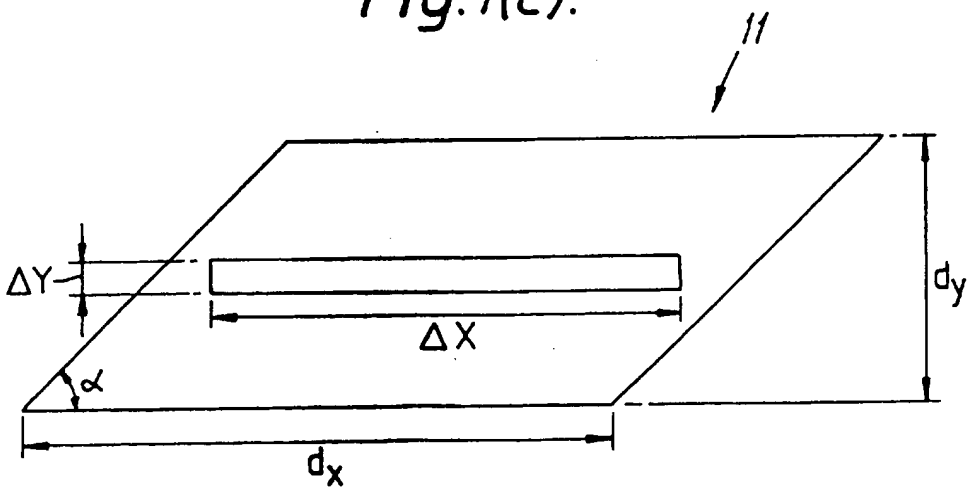

Fig. 2.

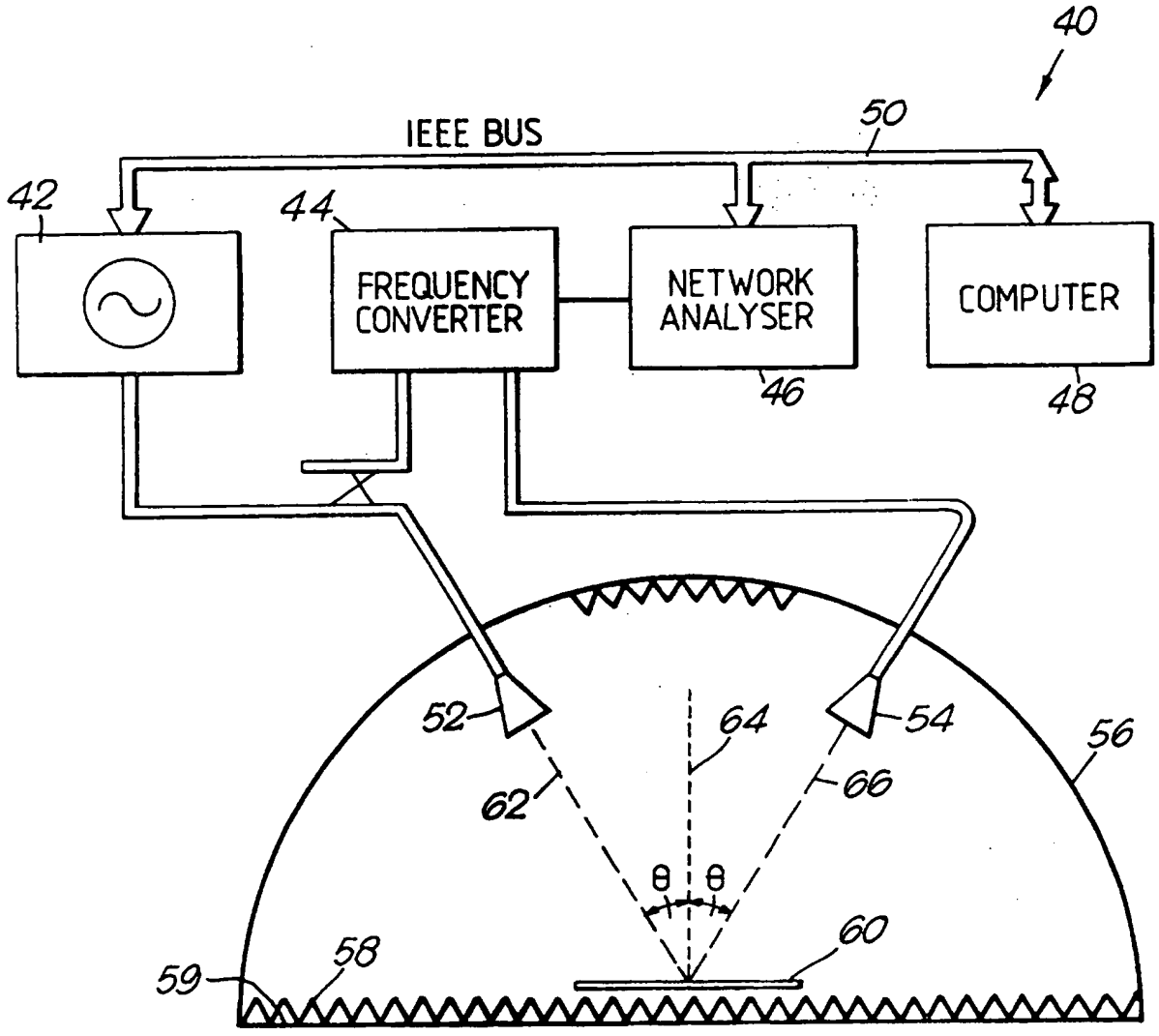
40
IEEE BUS
50
42
44
FREQUENCY CONVERTER
NETWORK ANALYSER
COMPUTER
46
48
52
54
56
64
62
66
θ
θ
58
59
60

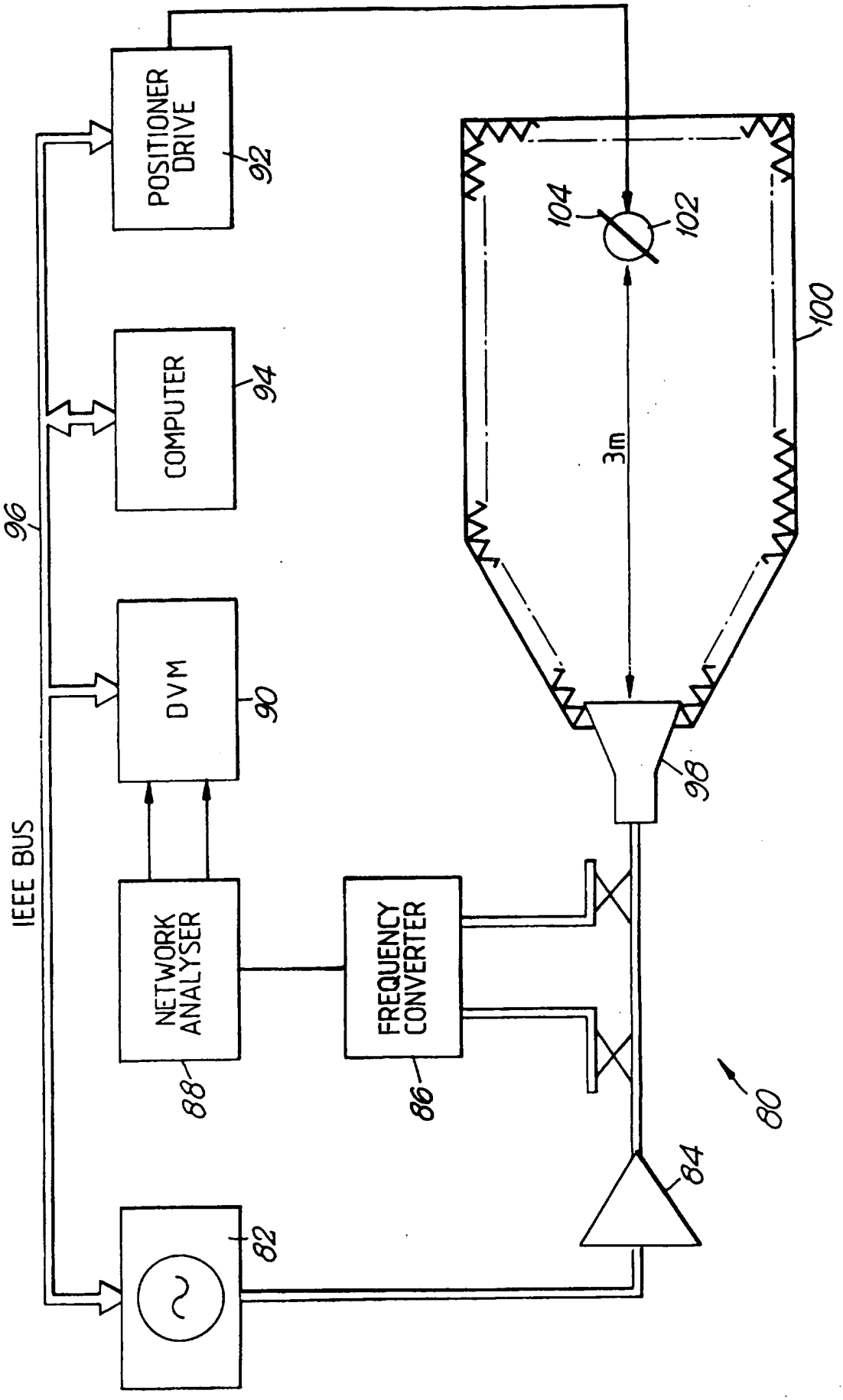
POSITIONER DRIVE
92
COMPUTER
94
96
DVM
90
IEEE BUS
NETWORK ANALYSER
88
FREQUENCY CONVERTER
86
82
84
80
98
100
104
102
3m

Fig. 3.

Fig. 4(a).

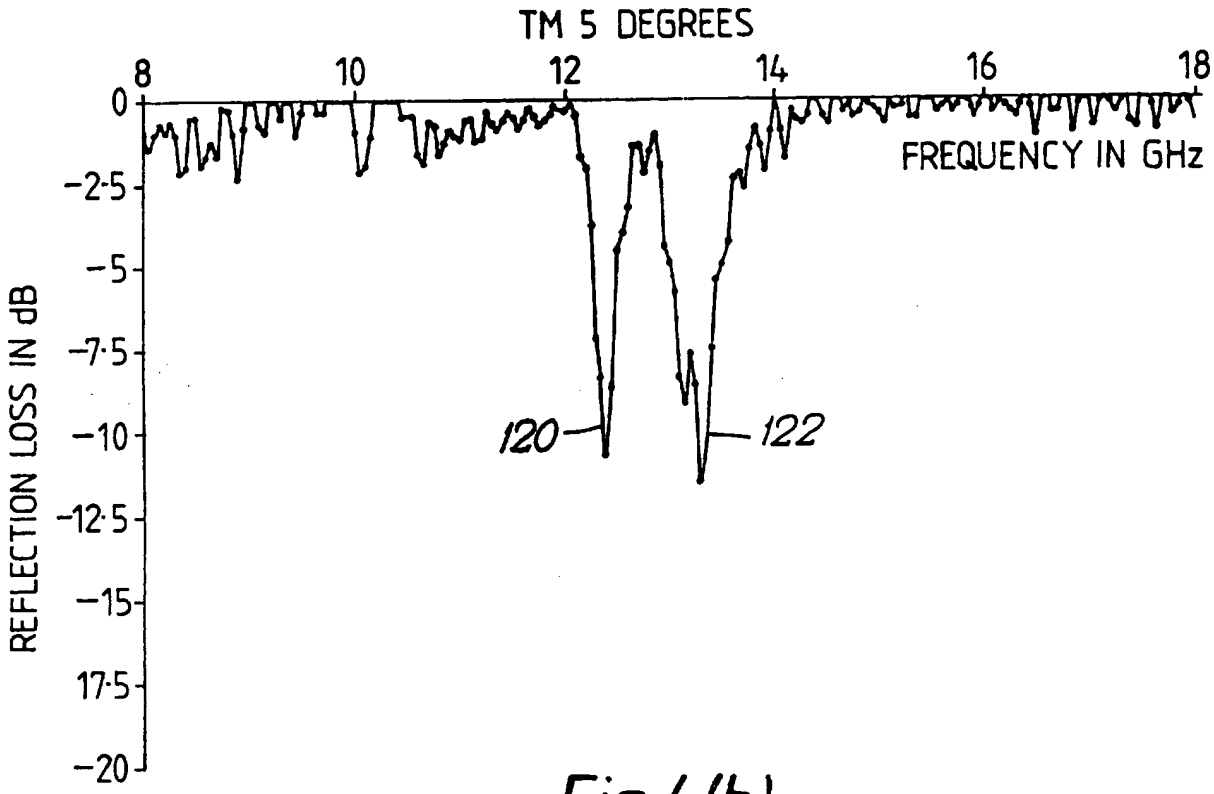
TM 5 DEGREES
8
10
12
14
16
18
0
-2·5
-5
-7·5
-10
-12·5
-15
17·5
-20
REFLECTION LOSS IN dB
FREQUENCY IN GHz
120
122

Fig. 4(b).

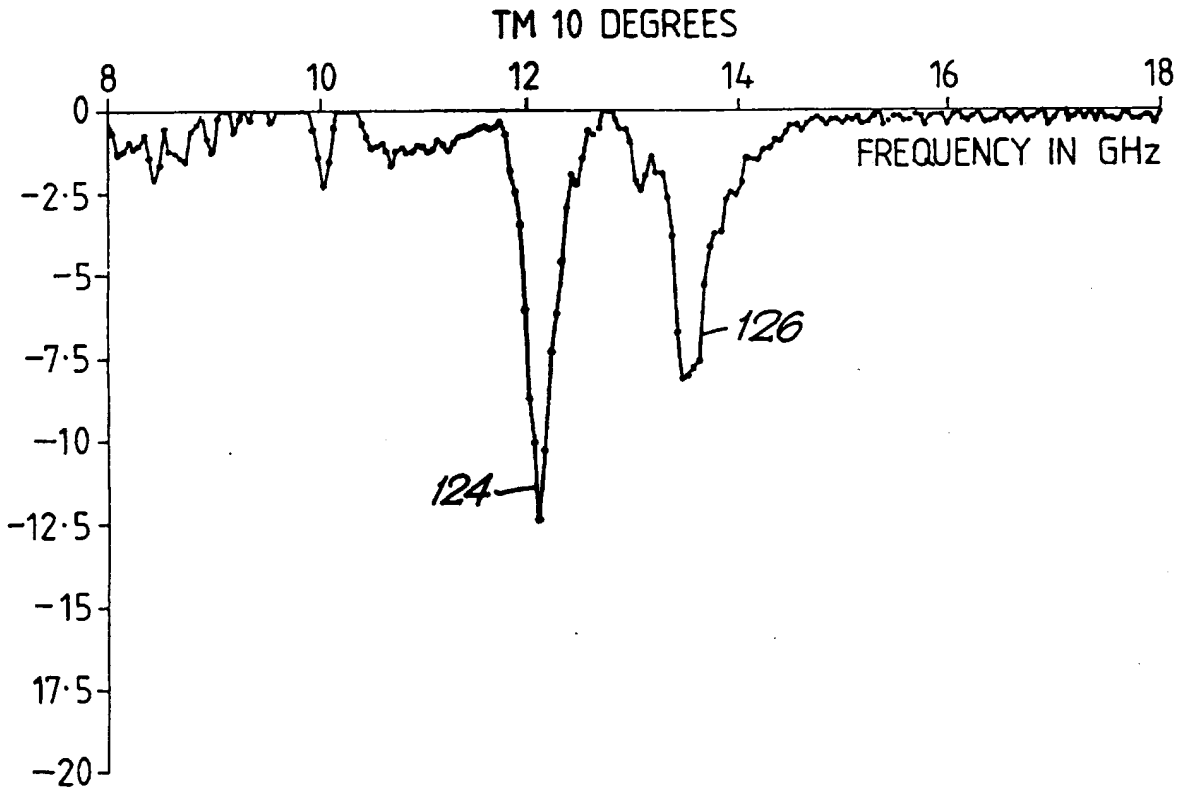
TM 10 DEGREES
8
10
12
14
16
18
0
-2·5
-5
-7·5
-10
-12·5
-15
17·5
-20
FREQUENCY IN GHz
124
126

Fig. 4(c).

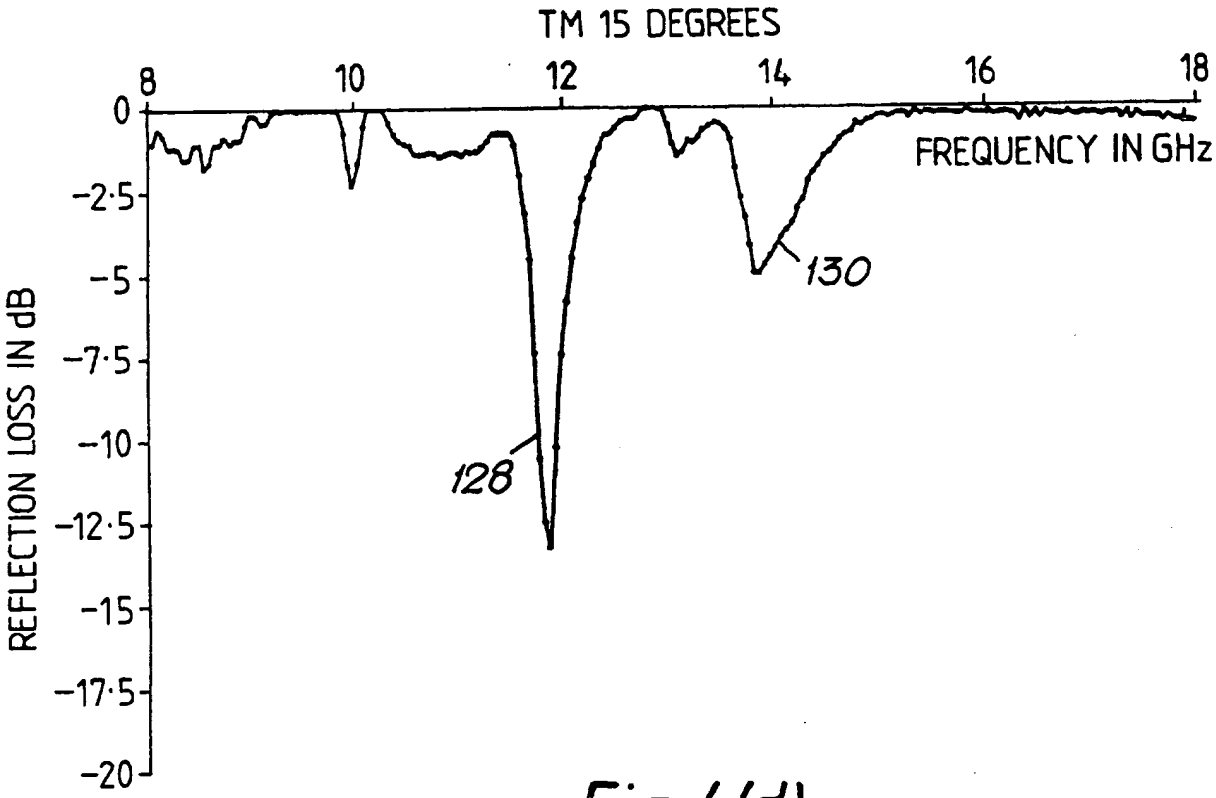
TM 15 DEGREES
8
10
12
14
16
18
0
-2·5
-5
-7·5
-10
-12·5
-15
-17·5
-20
REFLECTION LOSS IN dB
FREQUENCY IN GHz
128
130

Fig. 4(d).

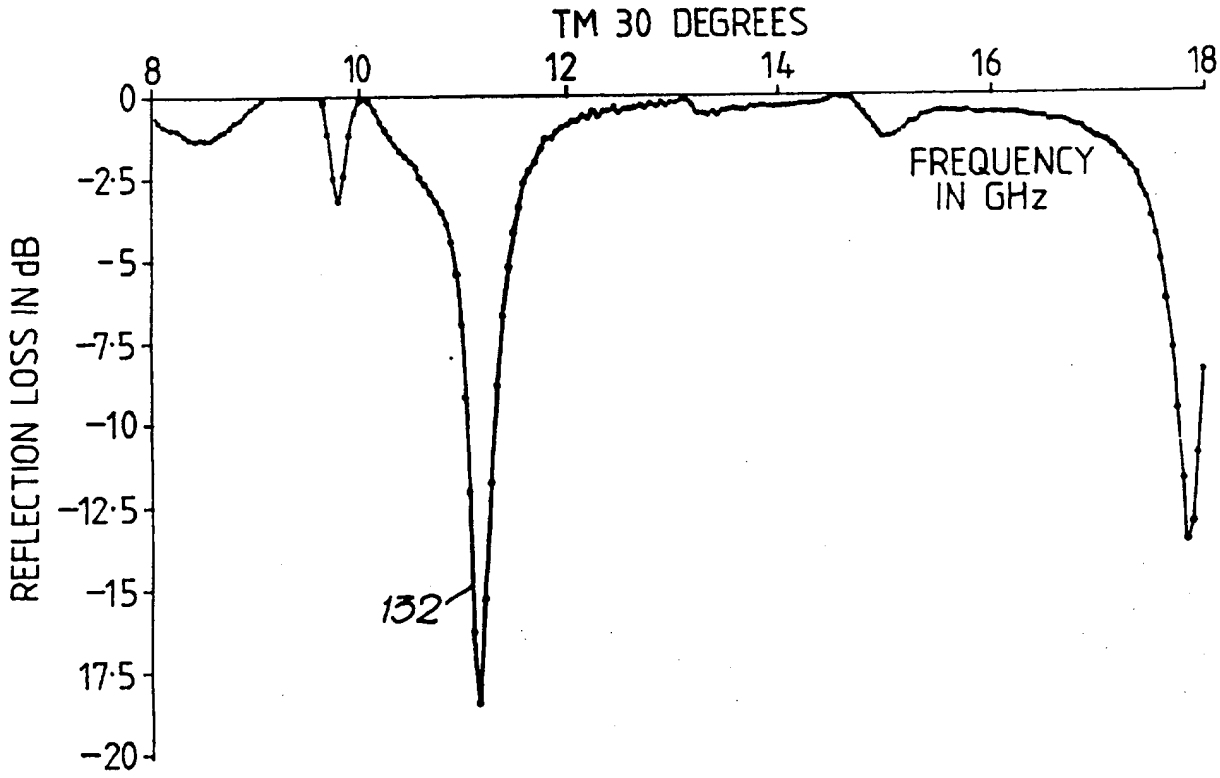
TM 30 DEGREES
8
10
12
14
16
18
0
-2·5
-5
-7·5
-10
-12·5
-15
17·5
-20
REFLECTION LOSS IN dB
FREQUENCY
IN GHz
132

Fig. 4(e).

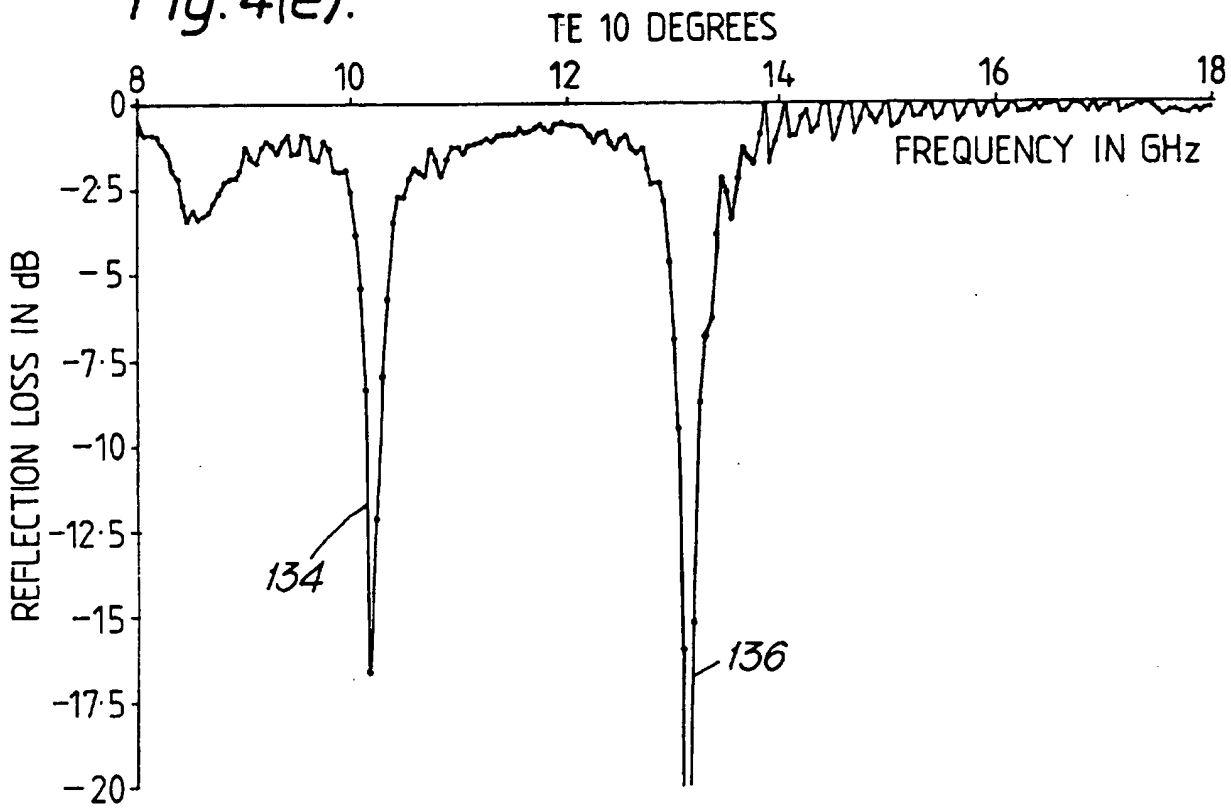
TE 10 DEGREES
8
10
12
14
16
18
0
-2·5
-5
-7·5
-10
-12·5
-15
-17·5
-20
REFLECTION LOSS IN dB
FREQUENCY IN GHz
134
136

Fig. 4(f).

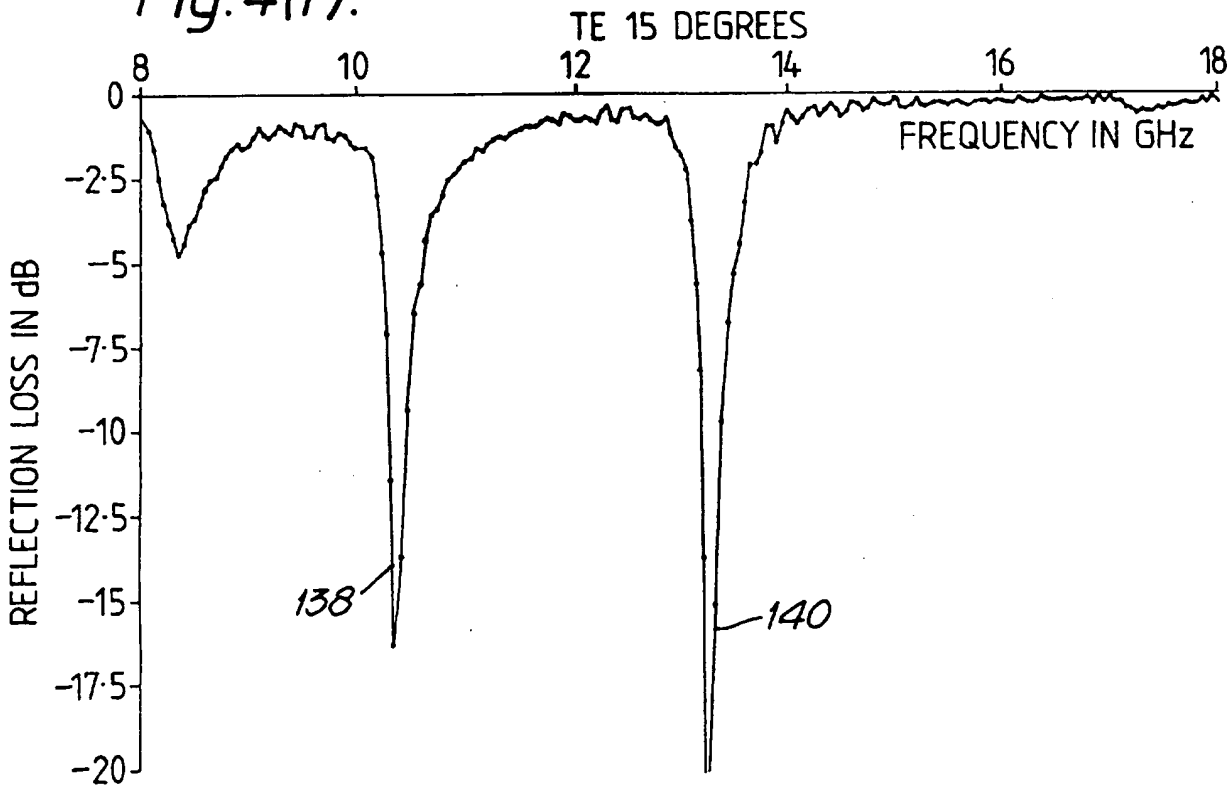
TE 15 DEGREES
8
10
12
14
16
18
0
-2·5
-5
-7·5
-10
-12·5
-15
-17·5
-20
REFLECTION LOSS IN dB
FREQUENCY IN GHz
138
140

Fig. 4(g).

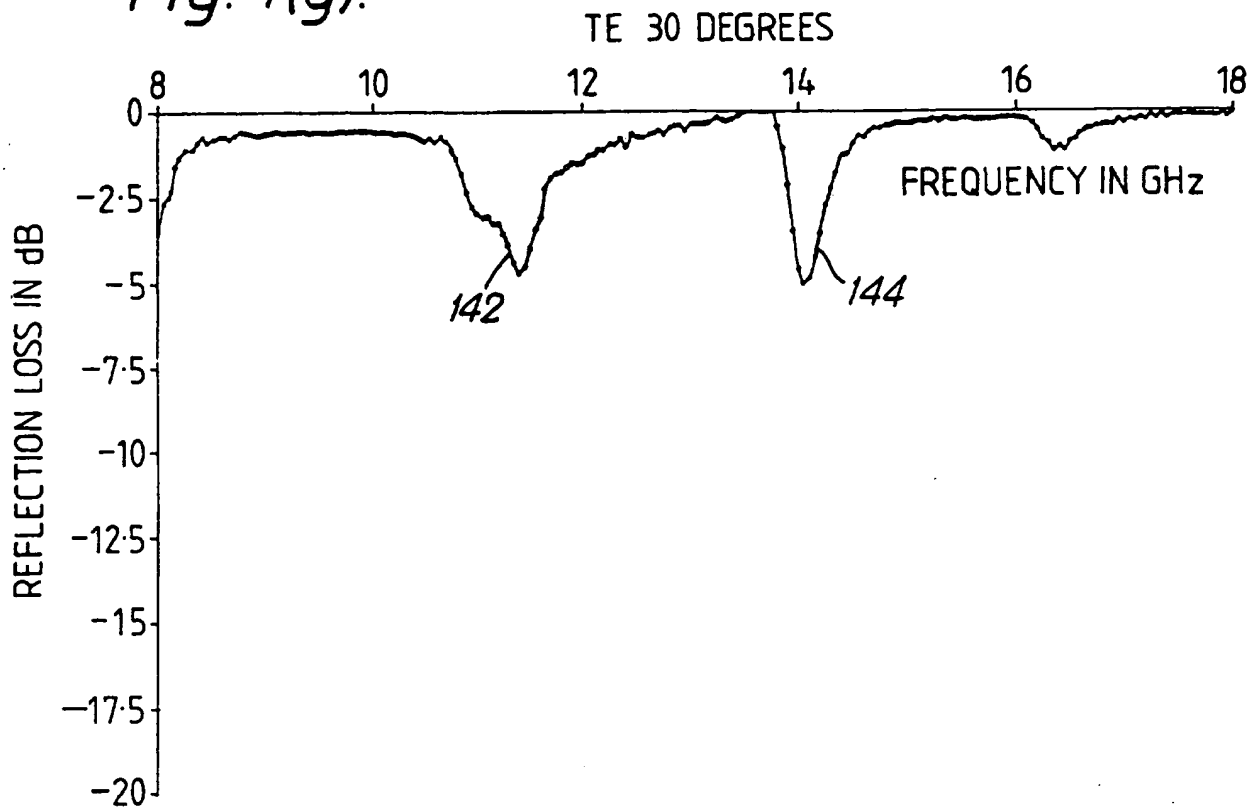
TE 30 DEGREES
8
10
12
14
16
18
0
-2·5
-5
-7·5
-10
-12·5
-15
-17·5
-20
REFLECTION LOSS IN dB
FREQUENCY IN GHz
142
144

Fig. 5(a).

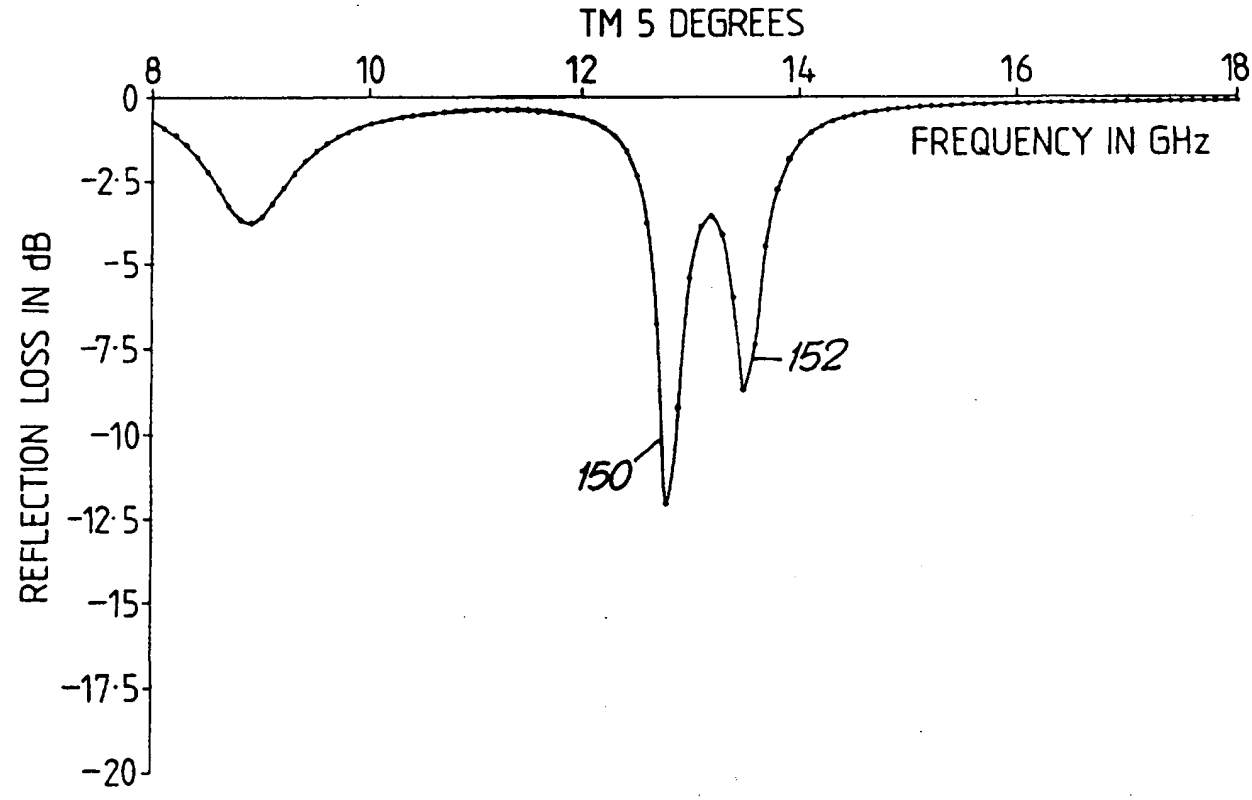
TM 5 DEGREES
8
10
12
14
16
18
0
-2·5
-5
-7·5
-10
-12·5
-15
-17·5
-20
REFLECTION LOSS IN dB
FREQUENCY IN GHz
150
152

Fig.5(b).

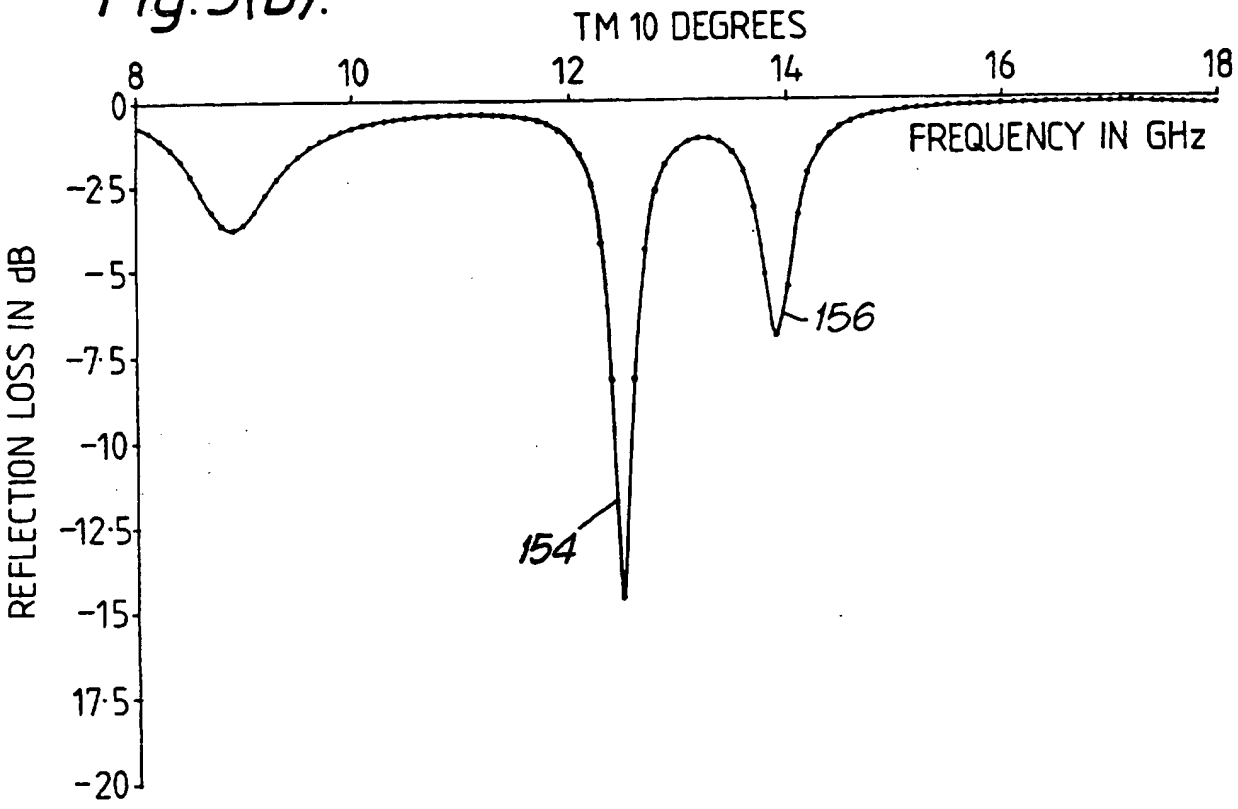
TM 10 DEGREES
8
10
12
14
16
18
0
-2·5
-5
-7·5
-10
-12·5
-15
17·5
-20
REFLECTION LOSS IN dB
FREQUENCY IN GHz
154
156

Fig.5(c).

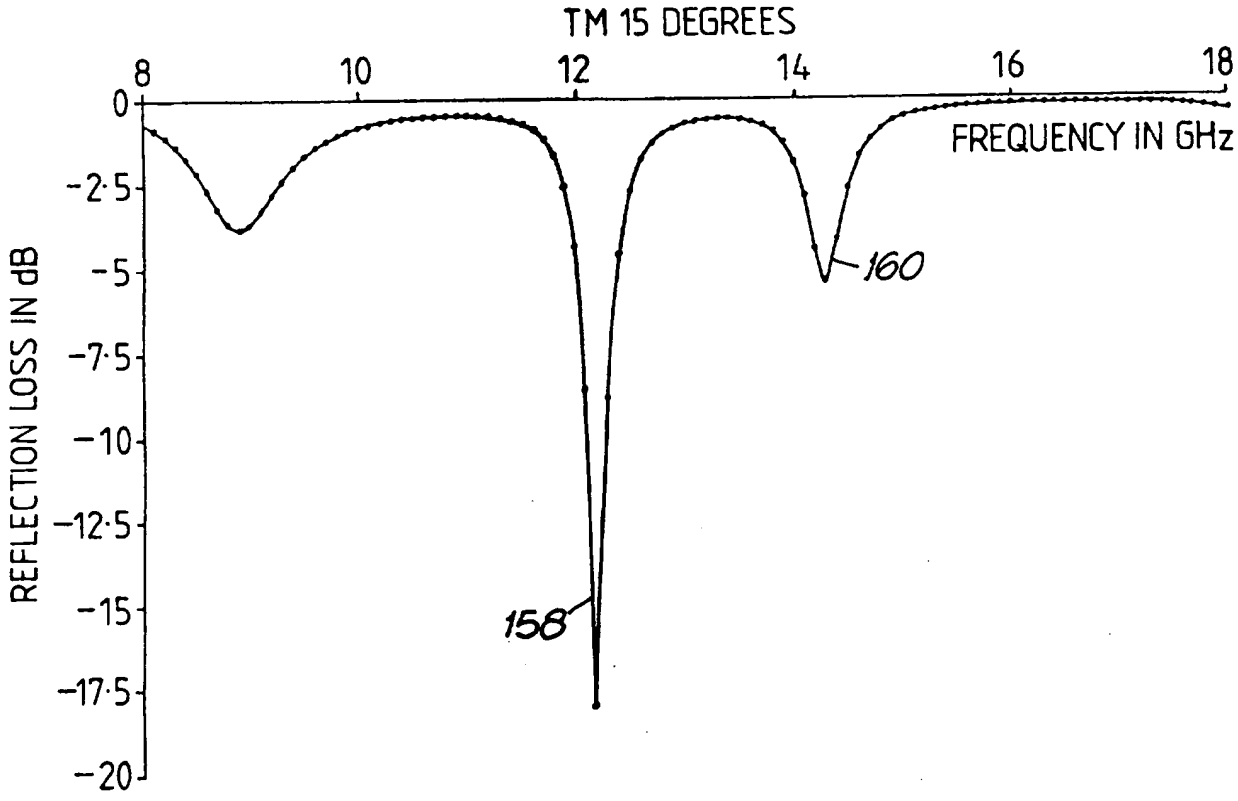
TM 15 DEGREES
8
10
12
14
16
18
0
-2·5
-5
-7·5
-10
-12·5
-15
-17·5
-20
REFLECTION LOSS IN dB
FREQUENCY IN GHz
158
160

Fig. 5(d).

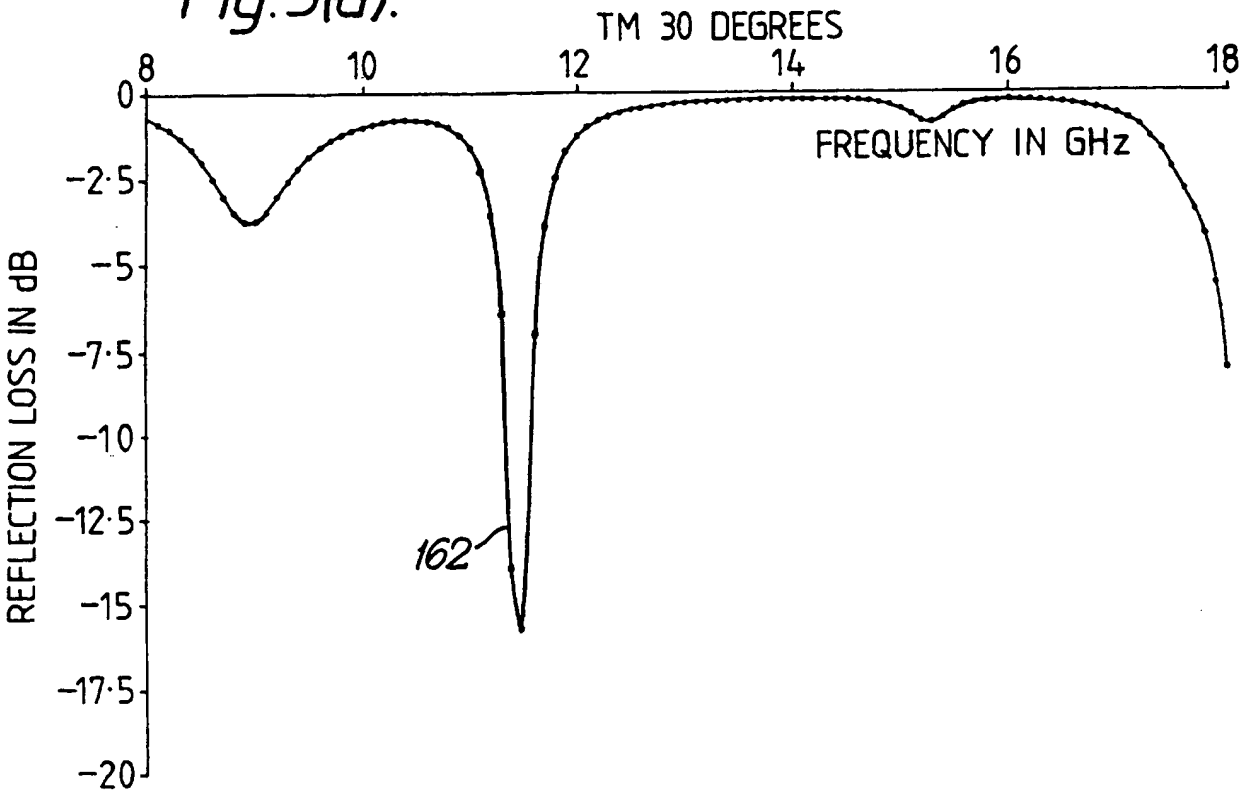
TM 30 DEGREES
8
10
12
14
16
18
0
-2·5
-5
-7·5
-10
-12·5
-15
-17·5
-20
REFLECTION LOSS IN dB
FREQUENCY IN GHz
162

Fig. 5(e).

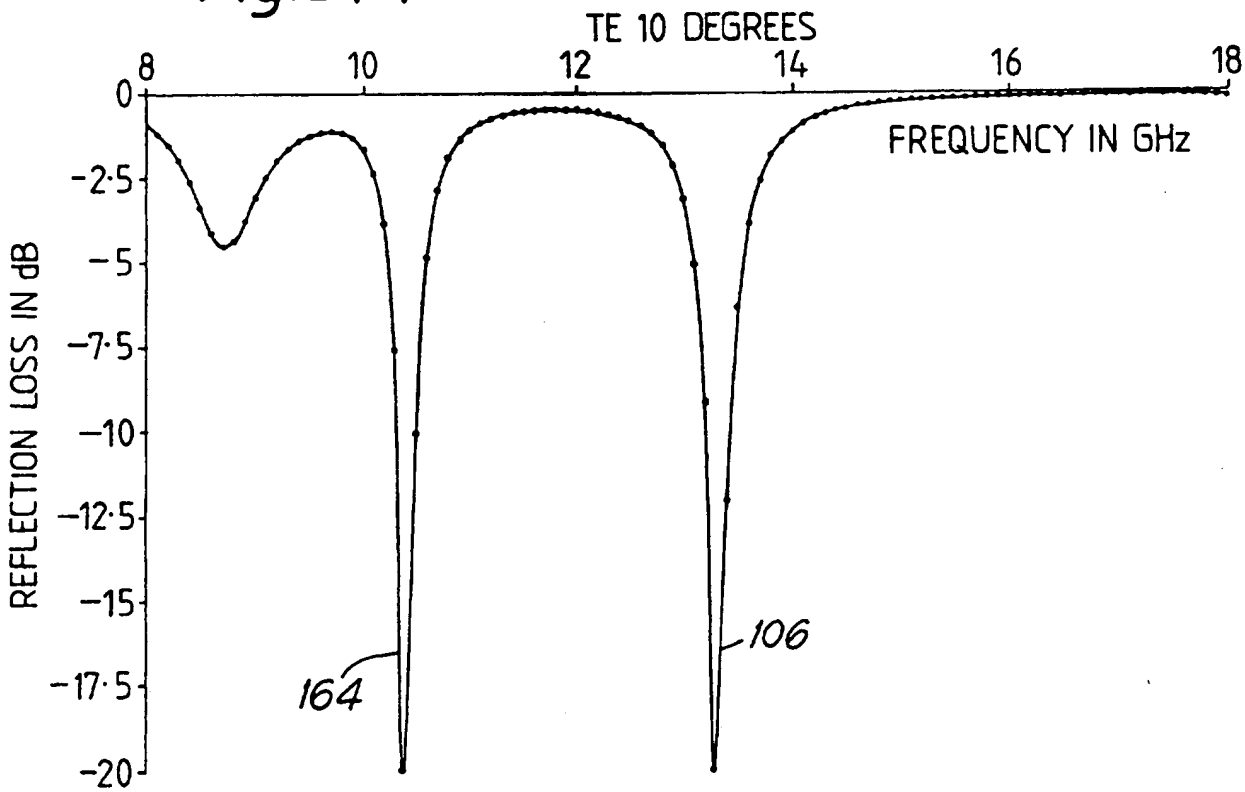
TE 10 DEGREES
8
10
12
14
16
18
0
-2·5
-5
-7·5
-10
-12·5
-15
-17·5
-20
REFLECTION LOSS IN dB
FREQUENCY IN GHz
164
106

Fig.5(f).

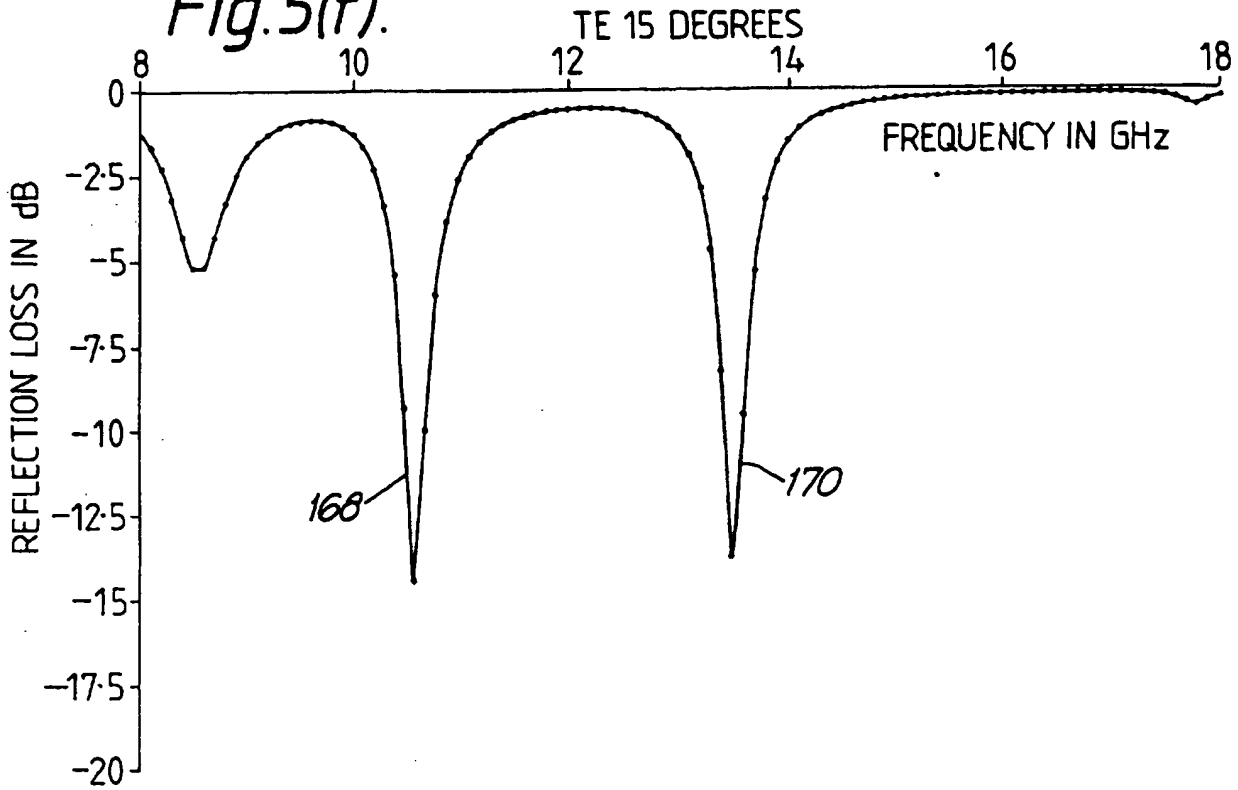
TE 15 DEGREES
8
10
12
14
16
18
0
-2·5
-5
-7·5
-10
-12·5
-15
-17·5
-20
REFLECTION LOSS IN dB
FREQUENCY IN GHz
168
170

Fig.5(g).

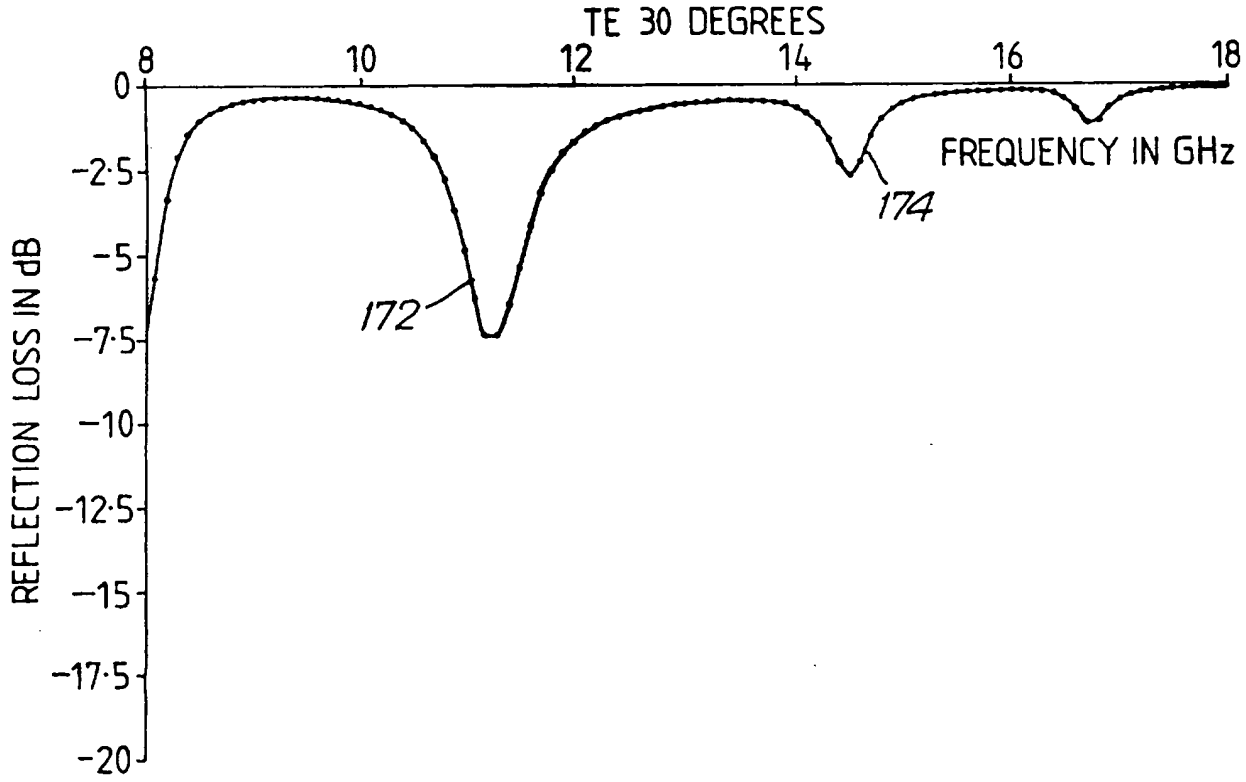
TE 30 DEGREES
8
10
12
14
16
18
0
-2·5
-5
-7·5
-10
-12·5
-15
-17·5
-20
REFLECTION LOSS IN dB
FREQUENCY IN GHz
172
174

Fig. 6.

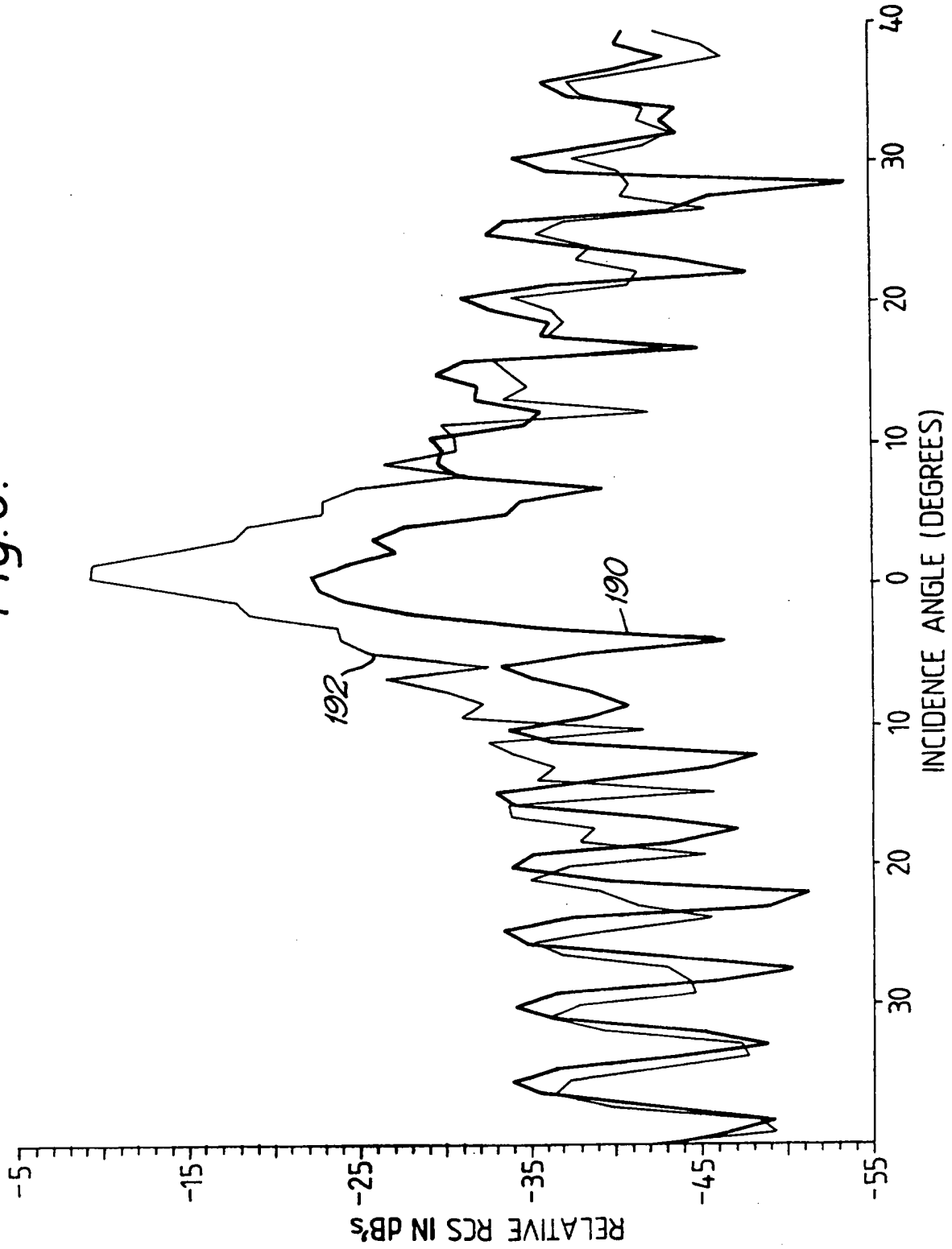
RELATIVE RCS IN dB's
-5
-15
-25
-35
-45
-55
INCIDENCE ANGLE (DEGREES)
40
30
20
10
0
10
20
30
190
192

Fig.7(a).

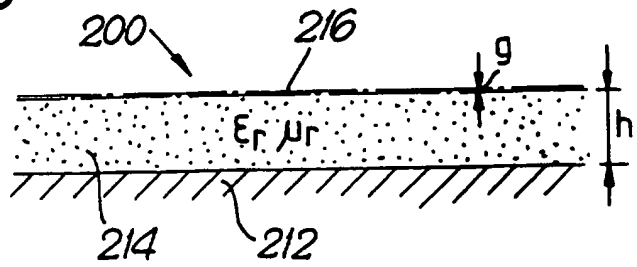

Fig.7(b).

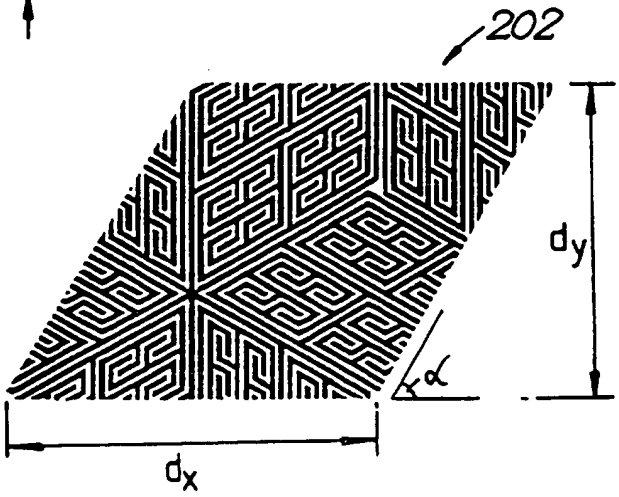

Fig.7(d).

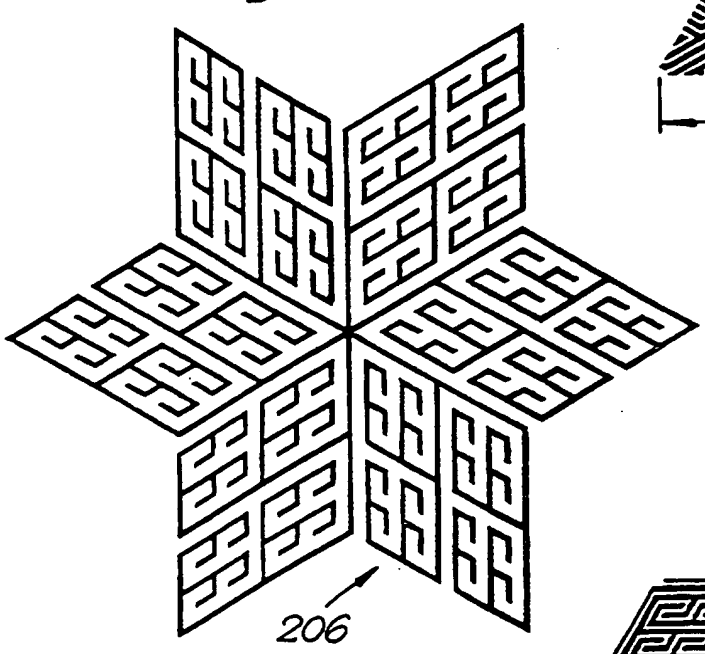

Fig.7(c).

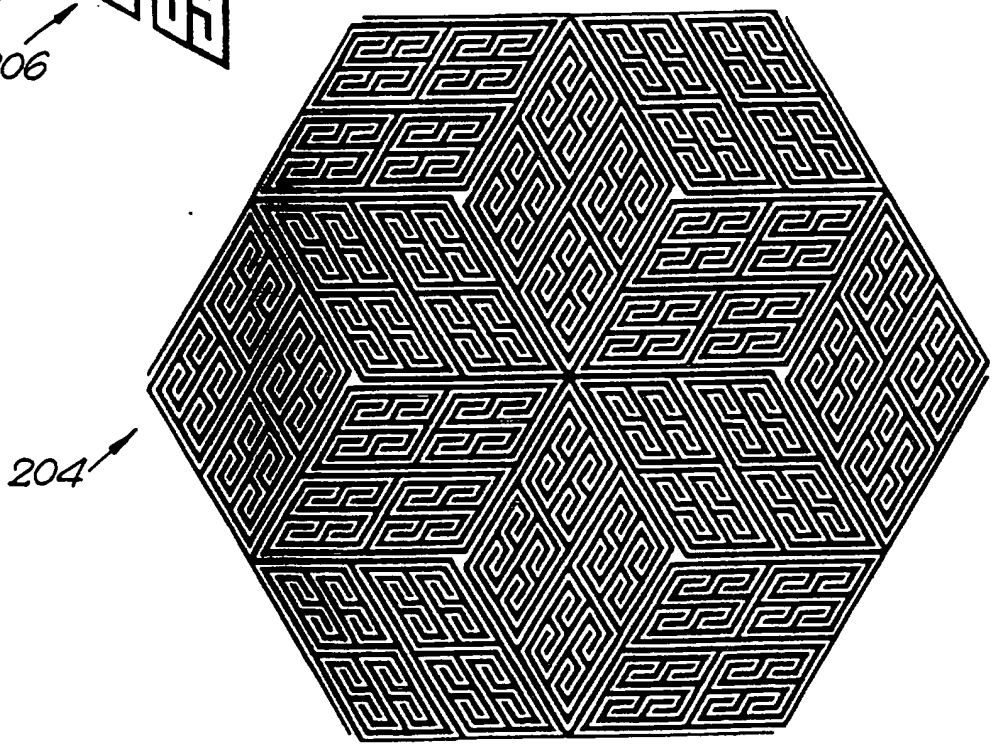

Fig. 8.

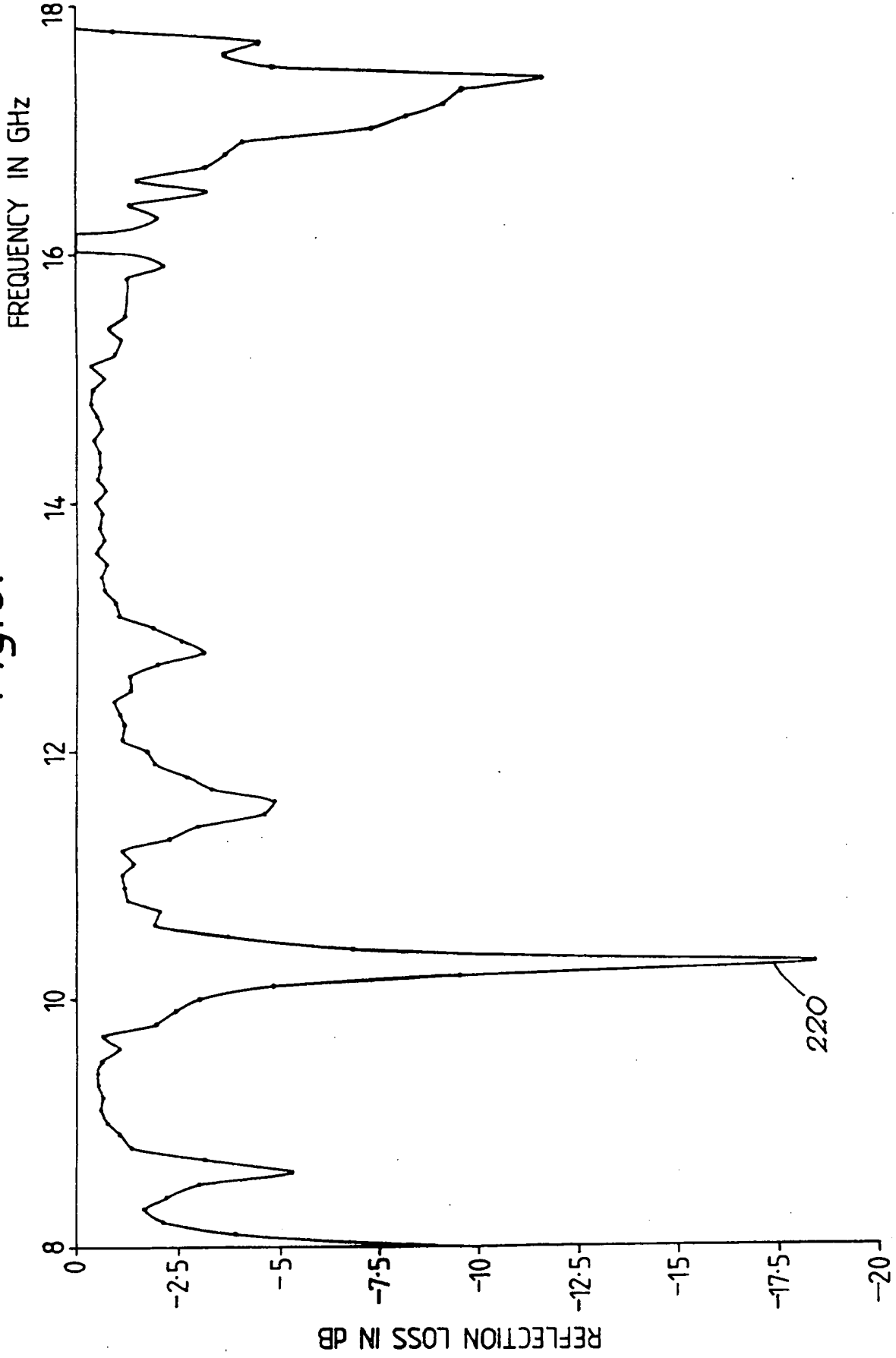
FREQUENCY IN GHz
8
10
12
14
16
18
REFLECTION LOSS IN dB
0
-2·5
-5
-7·5
-10
-12·5
-15
-17·5
-20
220

Fig. 9.

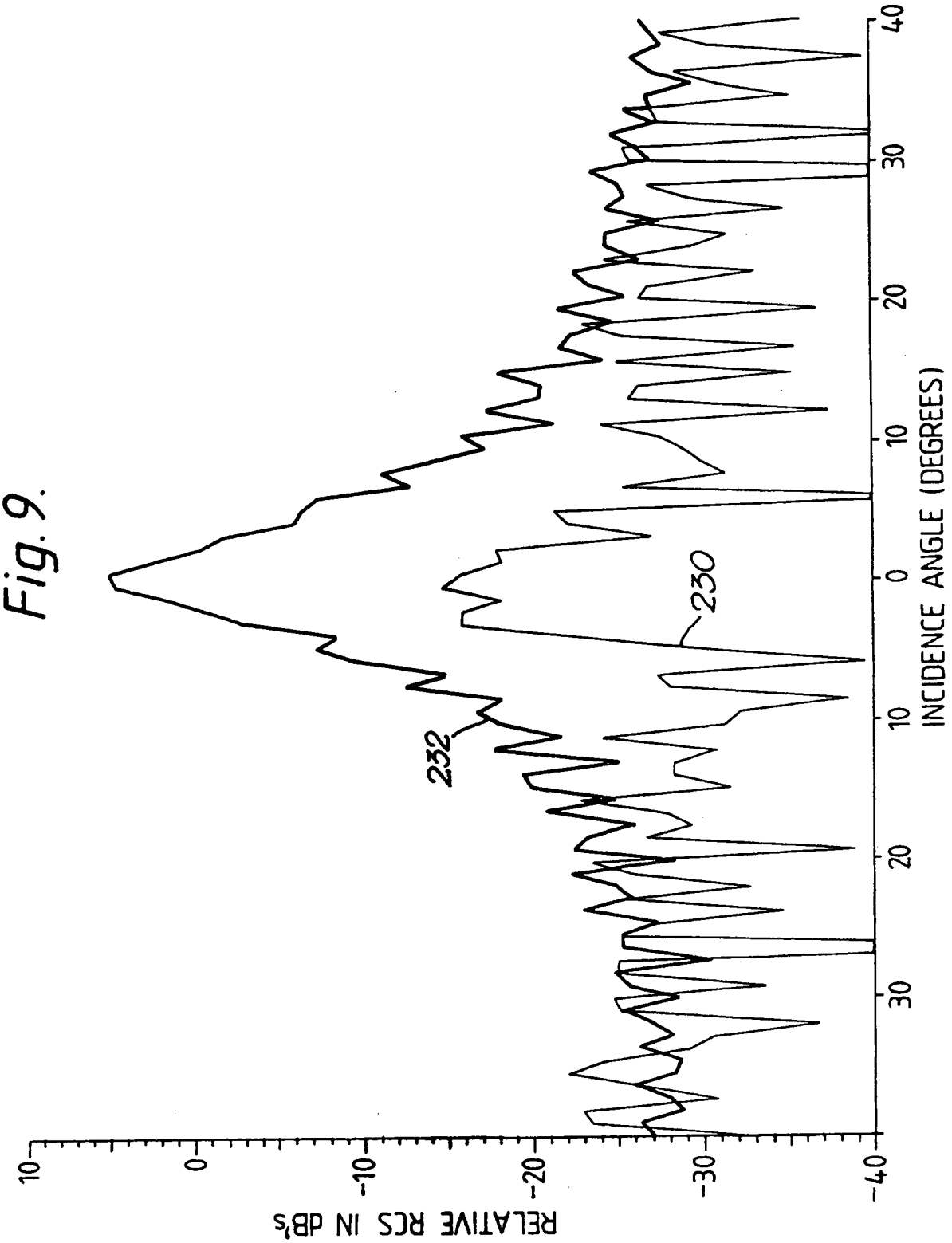
RELATIVE RCS IN dB's
10
0
-10
-20
-30
-40
40
30
20
10
0
10
20
30
INCIDENCE ANGLE (DEGREES)
230
232

Fig.10.

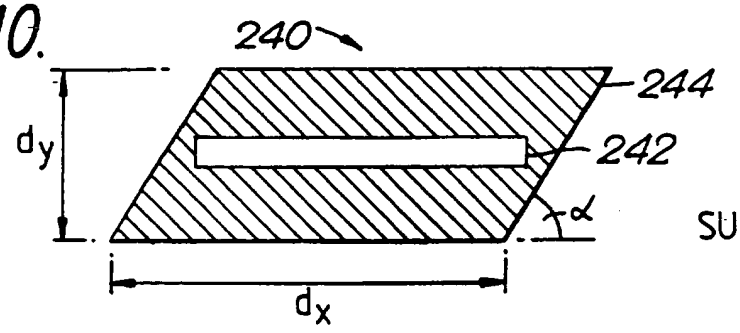

SUBSTRATE: $\mu_r = 2{\cdot}0 - j0{\cdot}864$
$\varepsilon_r = 1{\cdot}0$

Fig.11.

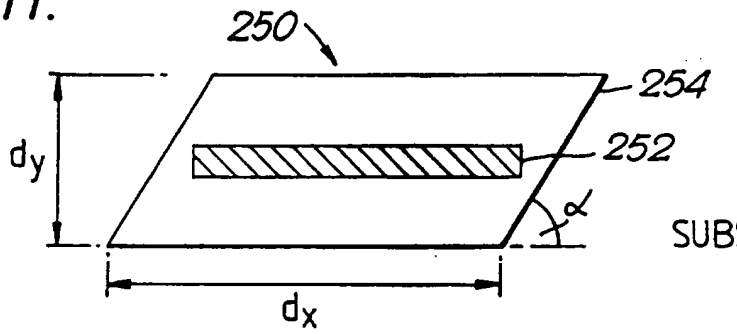

SUBSTRATE: $\mu_r = 2{\cdot}0 - j0{\cdot}864$
$\varepsilon_r = 1{\cdot}0$

Fig.12.

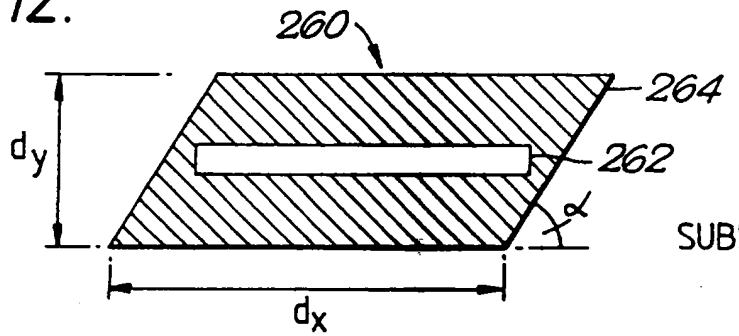

SUBSTRATE: $\varepsilon_r = 2{\cdot}0 - j0{\cdot}432$
$\mu_r = 1{\cdot}0$

Fig.13.

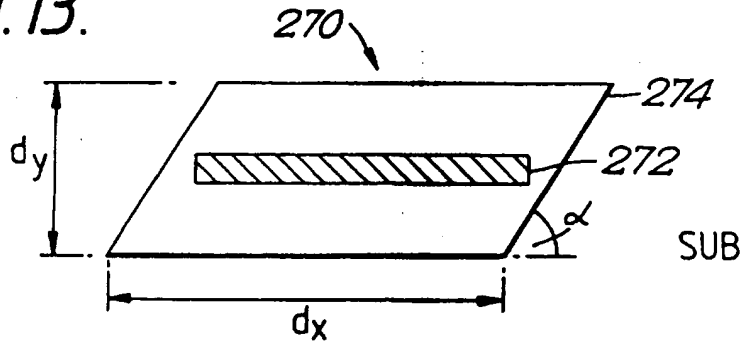

SUBSTRATE: $\varepsilon_r = 2{\cdot}0 - j0{\cdot}432$
$\mu_r = 1{\cdot}0$

Fig. 14(a).

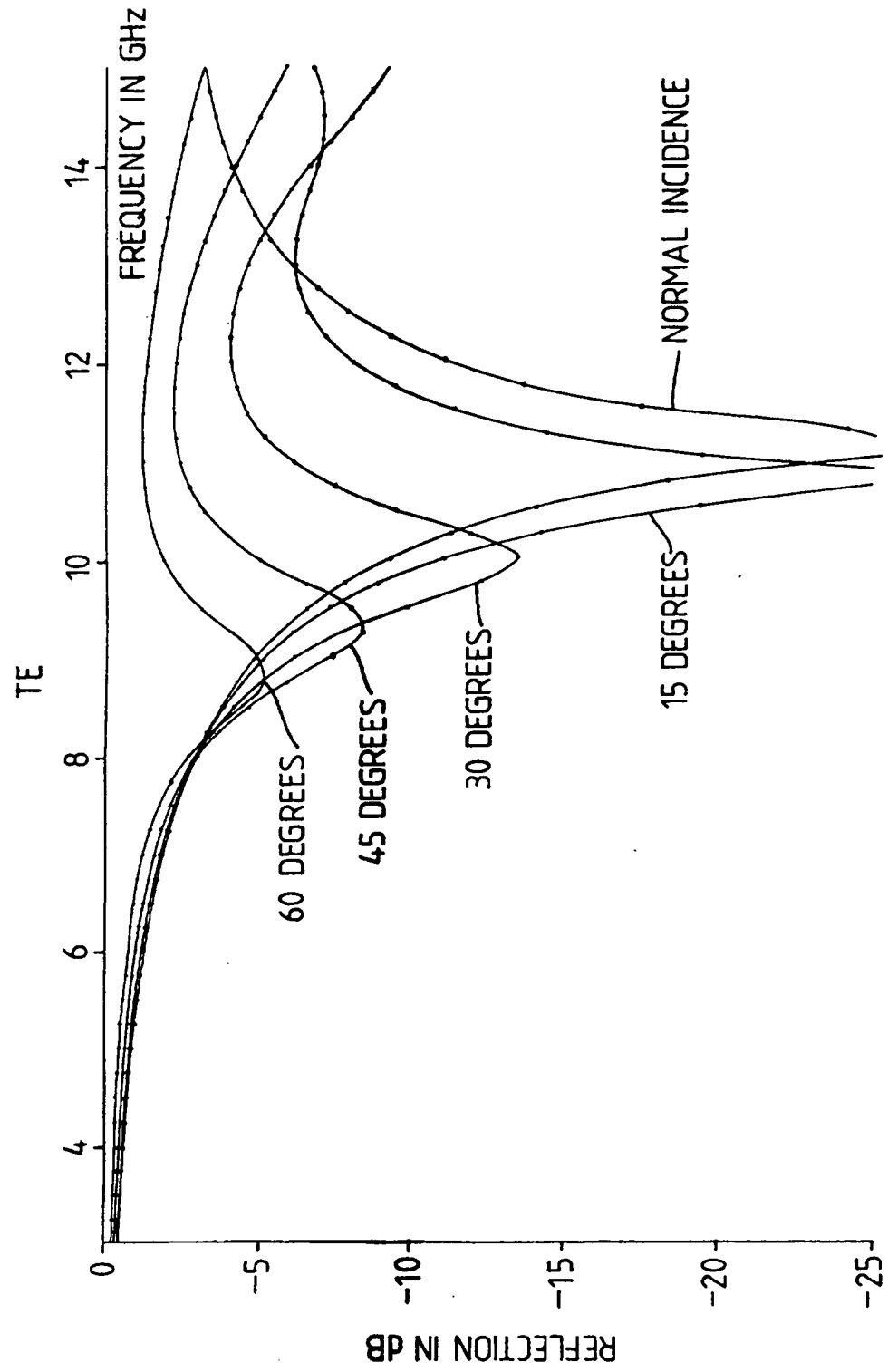
TE
FREQUENCY IN GHz
0
4
6
8
10
12
14
-5
-10
-15
-20
-25
REFLECTION IN dB
NORMAL INCIDENCE
15 DEGREES
30 DEGREES
45 DEGREES
60 DEGREES

Fig. 14(b).

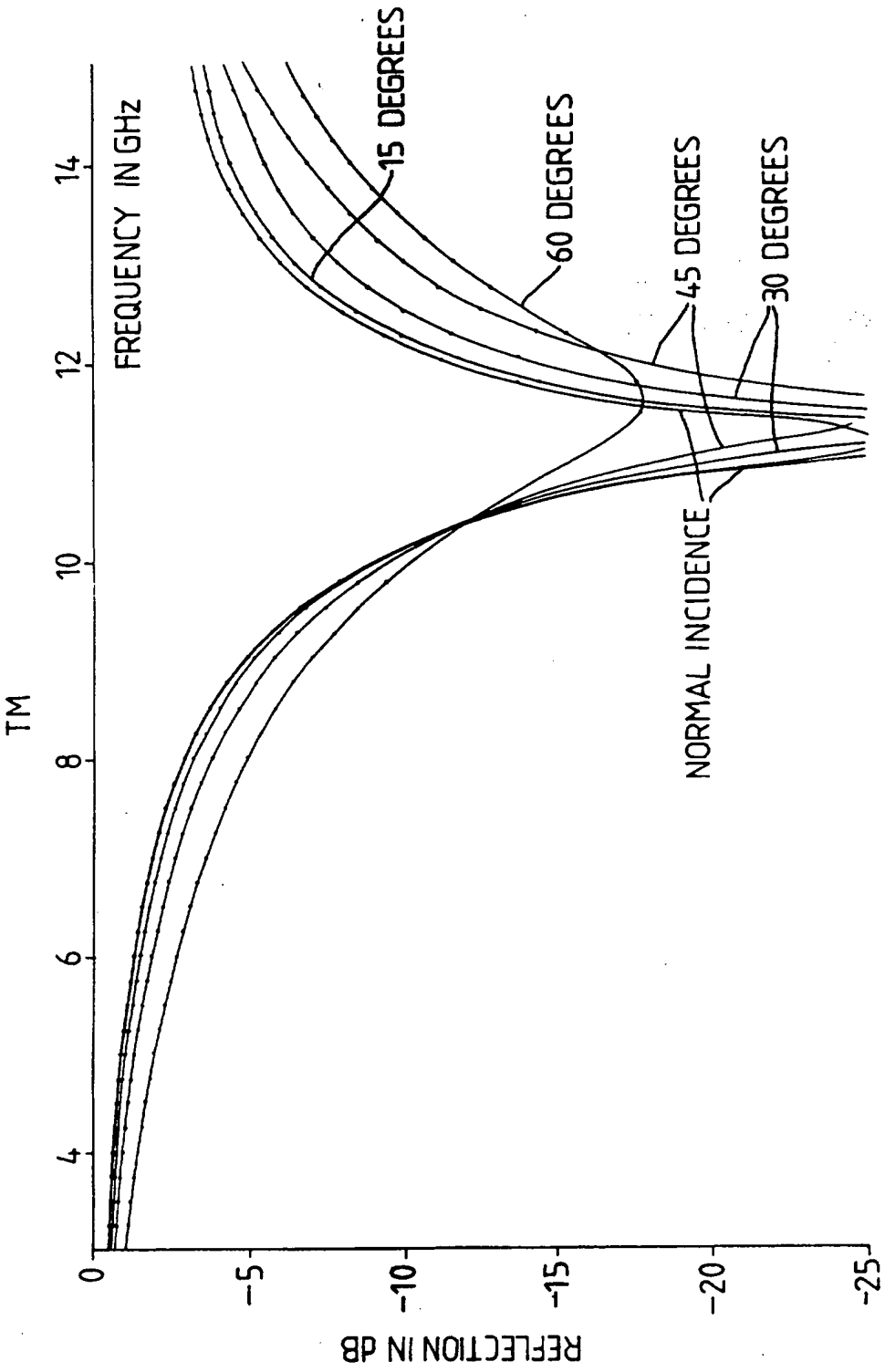
TM
FREQUENCY IN GHz
REFLECTION IN dB
0
4
6
8
10
12
14
-5
-10
-15
-20
-25
15 DEGREES
60 DEGREES
45 DEGREES
30 DEGREES
NORMAL INCIDENCE

Fig. 15(a).

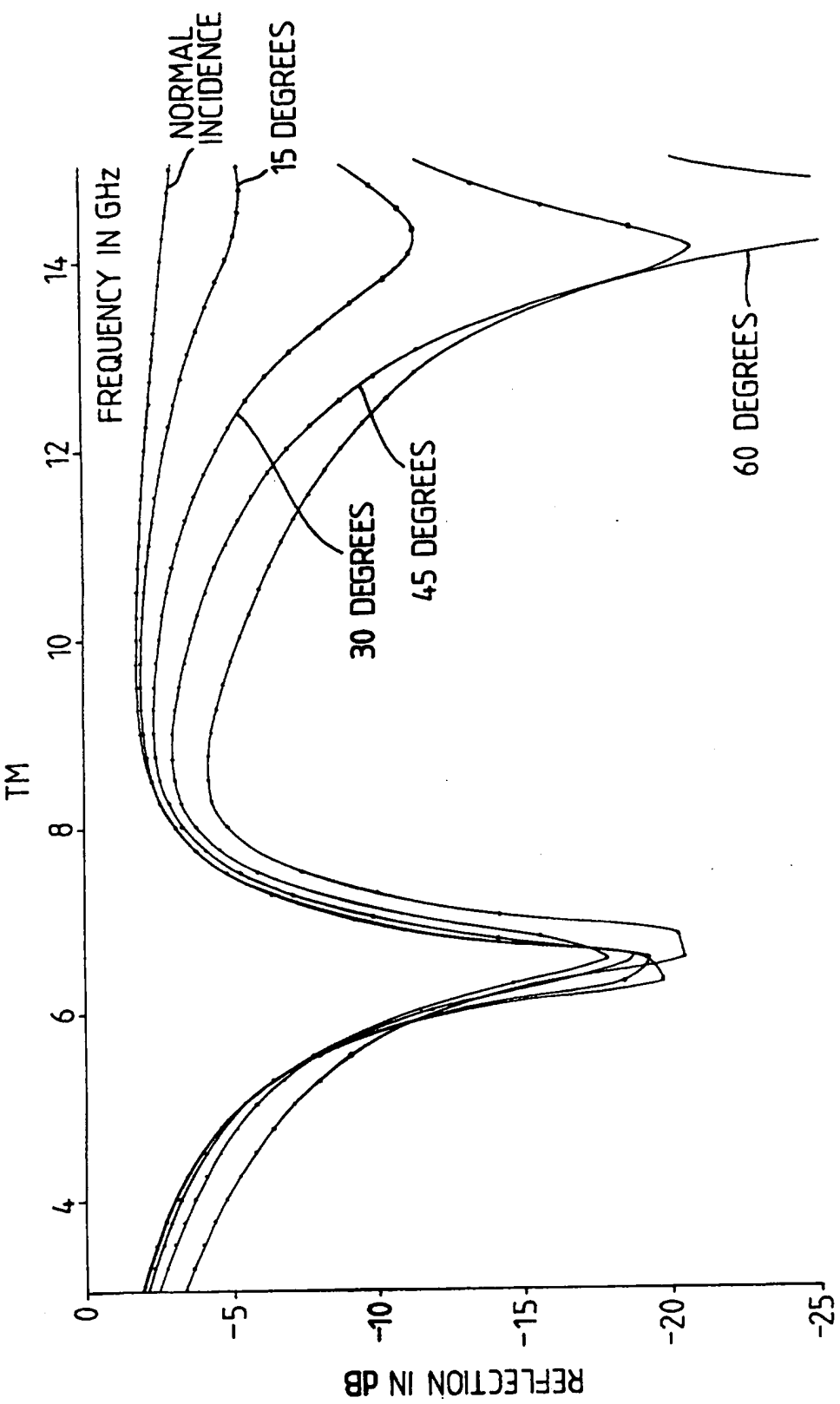
TM
FREQUENCY IN GHz
REFLECTION IN dB
NORMAL INCIDENCE
15 DEGREES
30 DEGREES
45 DEGREES
60 DEGREES
0
4
6
8
10
12
14
-5
-10
-15
-20
-25

Fig.15(b).

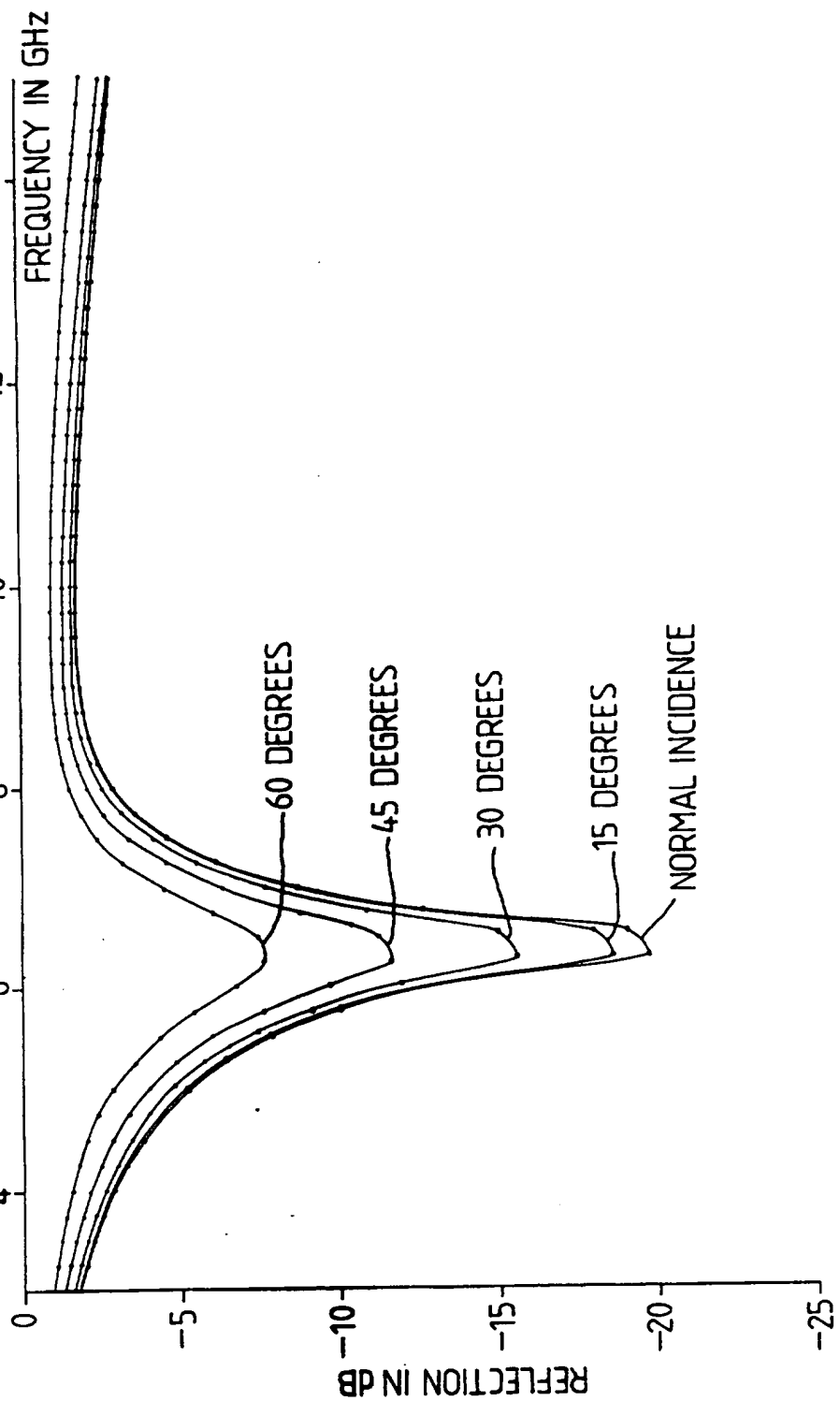
TE
FREQUENCY IN GHz
4
6
8
10
12
14
0
-5
-10
-15
-20
-25
REFLECTION IN dB
60 DEGREES
45 DEGREES
30 DEGREES
15 DEGREES
NORMAL INCIDENCE

Fig. 16(a).

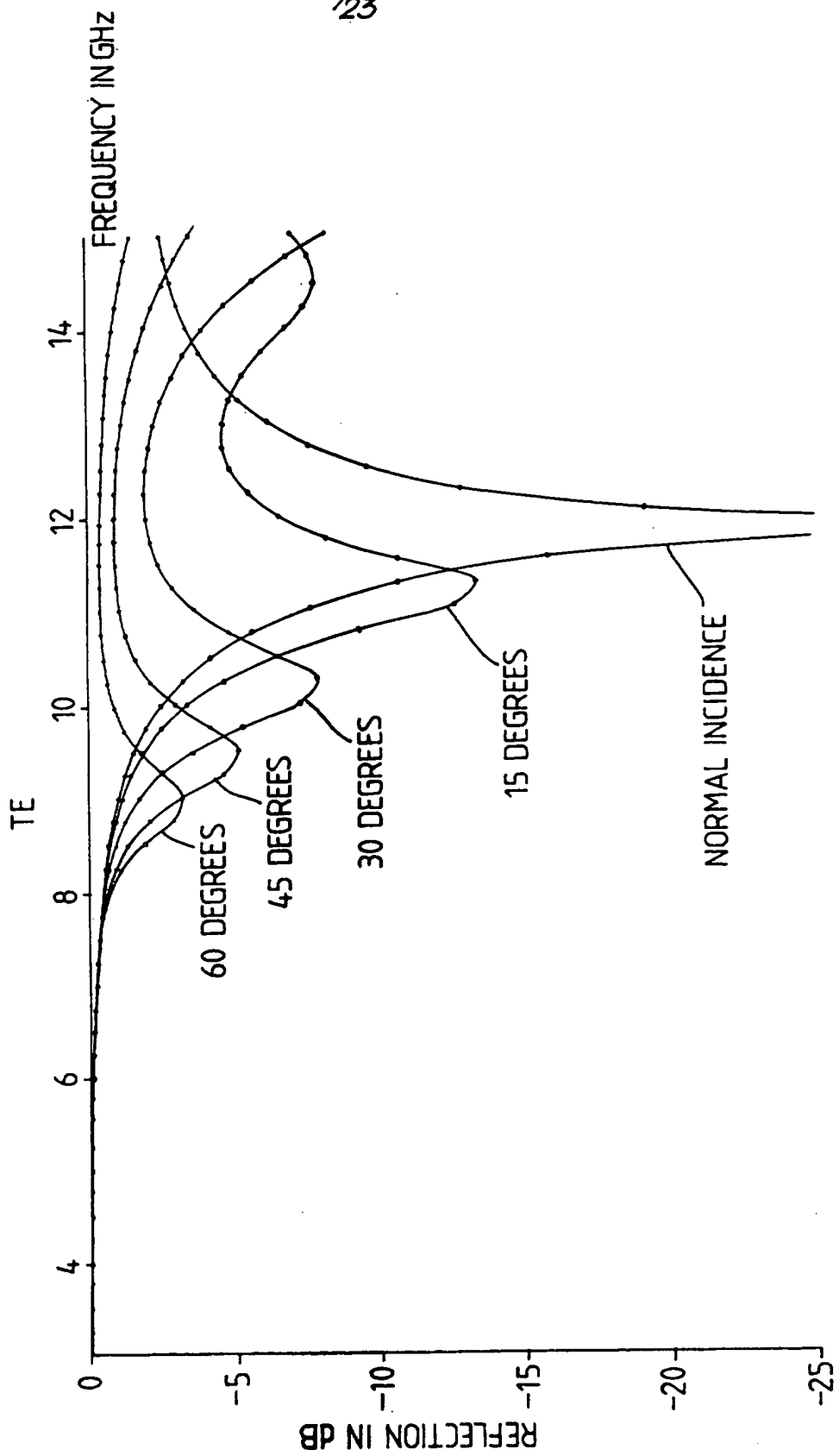
FREQUENCY IN GHz
TE
REFLECTION IN dB
0
-5
-10
-15
-20
-25
4
6
8
10
12
14
60 DEGREES
45 DEGREES
30 DEGREES
15 DEGREES
NORMAL INCIDENCE

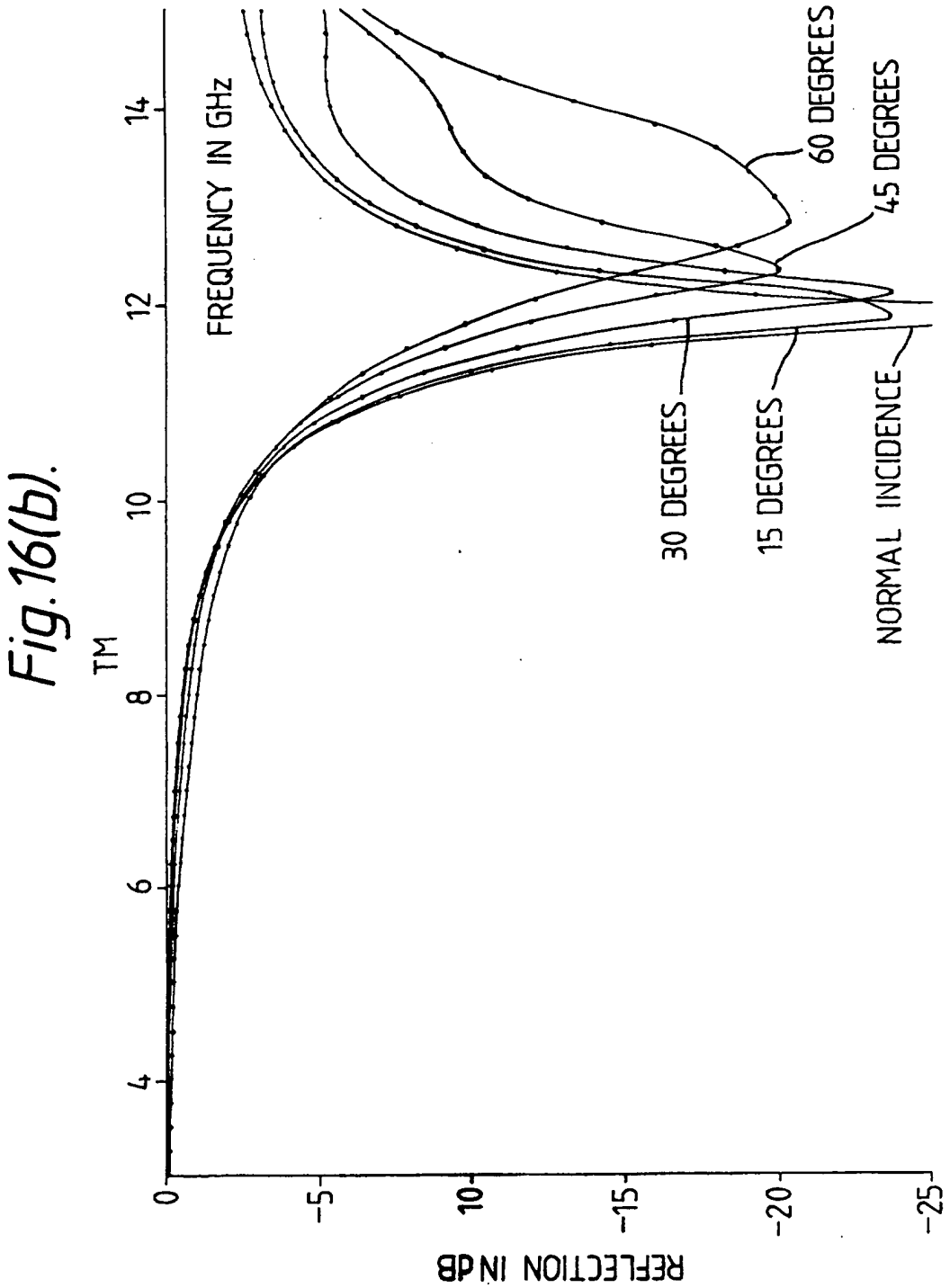
REFLECTION IN dB
0
-5
-10
-15
-20
-25
4
6
8
10
12
14
FREQUENCY IN GHz
TM
60 DEGREES
45 DEGREES
30 DEGREES
15 DEGREES
NORMAL INCIDENCE

Fig. 16(b).

Fig.17(a).

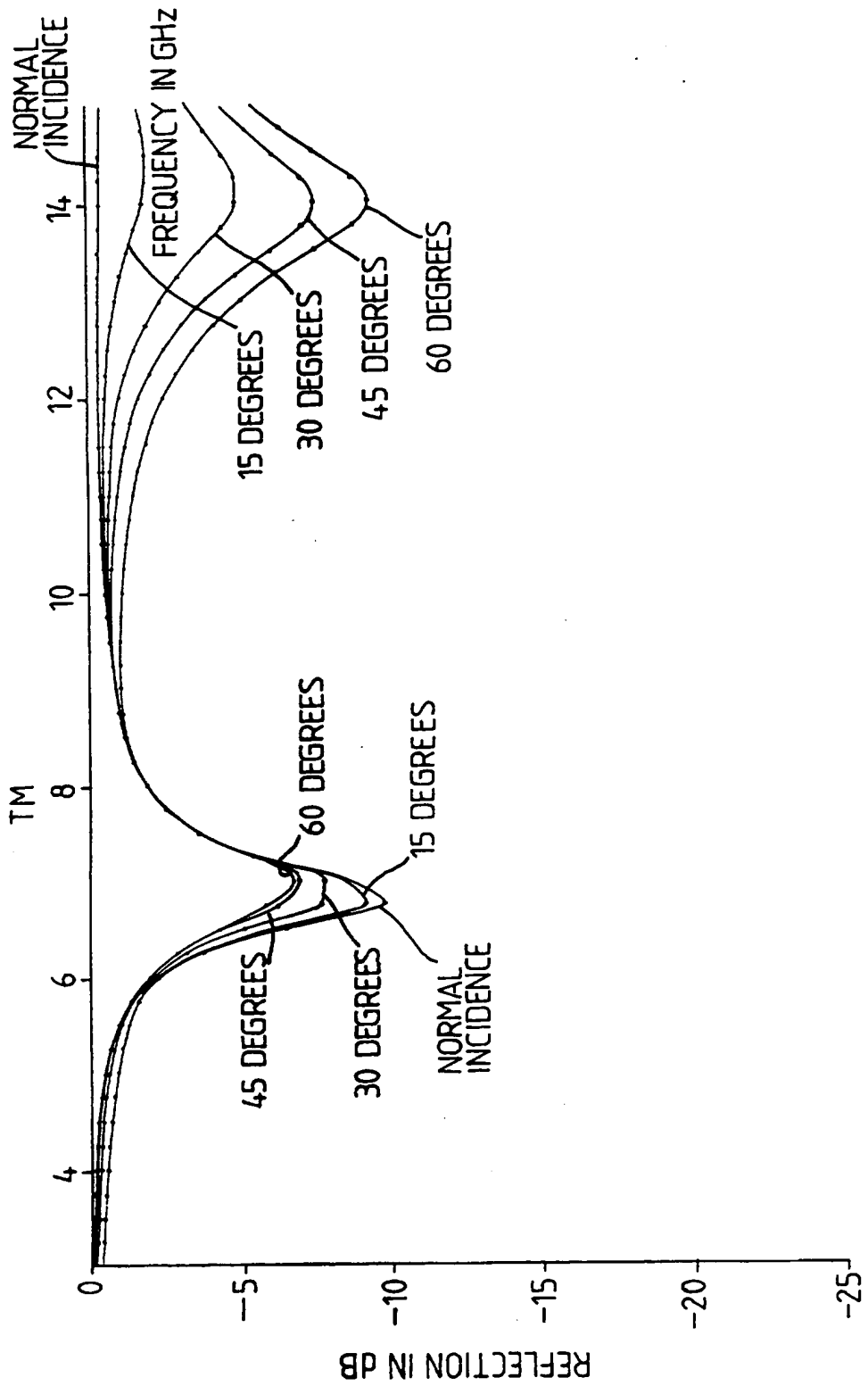
REFLECTION IN dB
0
-5
-10
-15
-20
-25
4
6
8
10
12
14
FREQUENCY IN GHz
TM
NORMAL INCIDENCE
15 DEGREES
30 DEGREES
45 DEGREES
60 DEGREES
60 DEGREES
15 DEGREES
45 DEGREES
30 DEGREES
NORMAL INCIDENCE

Fig.17(b).

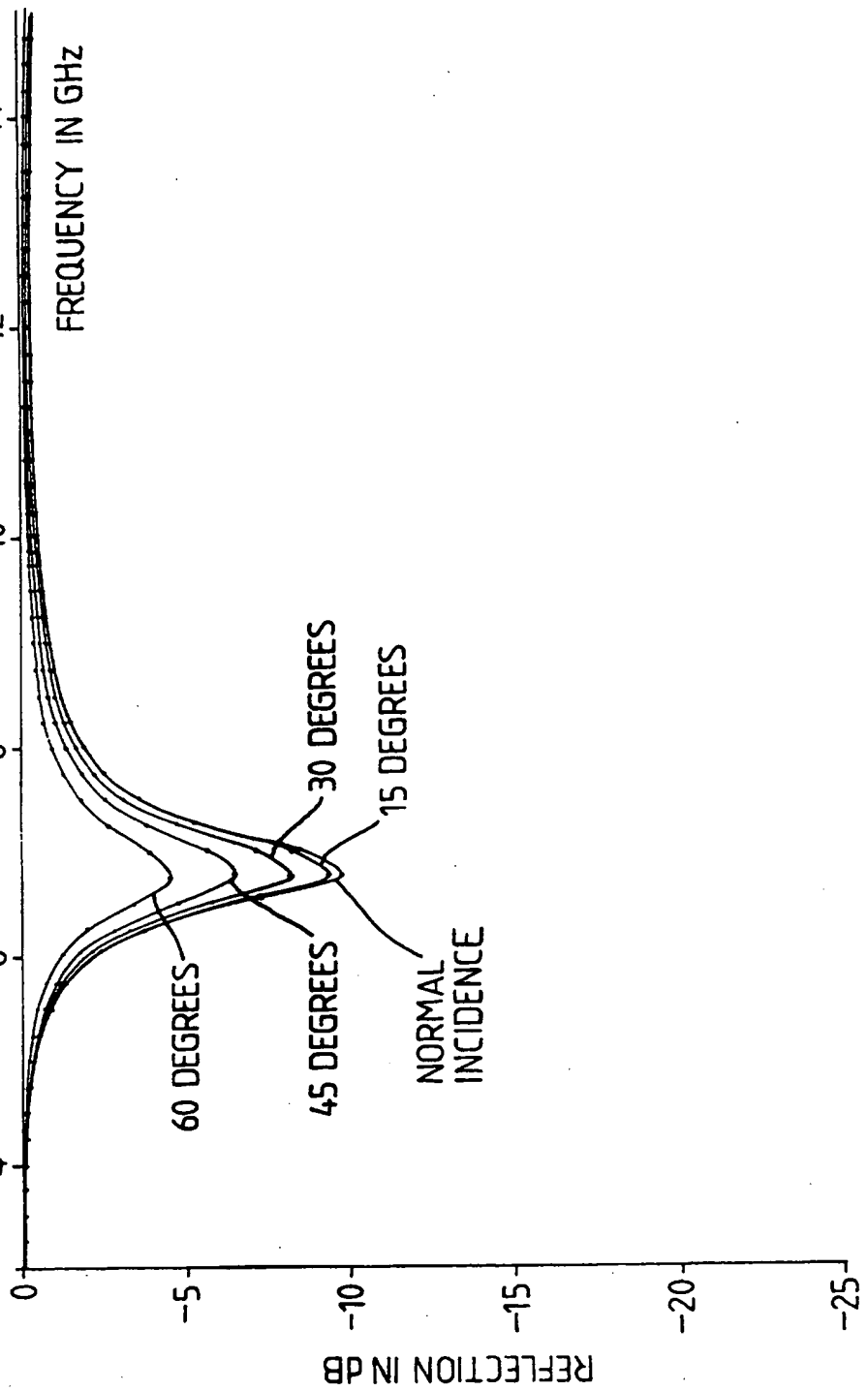
TE
FREQUENCY IN GHz
REFLECTION IN dB
0
4
6
8
10
12
14
-5
-10
-15
-20
-25
60 DEGREES
45 DEGREES
30 DEGREES
15 DEGREES
NORMAL INCIDENCE

2336472

FREQUENCY SELECTIVE RADAR ABSORBENT STRUCTURE

The invention relates to a frequency selective radar absorbent (FSRA) structure.

Frequency selective structures, (FSSs) are known in the prior art. They are often referred to as frequency selective surfaces. They may be active or passive. The passive variety, at its simplest, consists of periodic arrays of conducting, or impedance, elements, or slots in a conducting sheet. Active FSSs have periodic arrays of elements whose impedance may be altered by the application of a control voltage. Such passive or active FSSs are known in the prior art for use as a single layer or interleaved with dielectric layers to produce multi-layer structures. Some examples of passive multi-layered structures are discussed by R Orta, R Tascone and R Zich in IEE Proceedings, Vol 135, Pt H, No 2, (1988), pp 78-82.

Radar absorbent (RAb) materials are also known in the prior art. Some examples are described by E F Knott, J F Shaeffer and M T Tuley in "Radar Cross Section", Artech House Inc., Norwood, Mass, USA, (1985). These examples include Dallenbach Layers and Salisbury screens. Prior art RAb materials consist of single or multiple layers of lossy dielectric or magnetic material over a conducting layer. Prior art RAb materials are dependent on the materials having significant loss tangents. Loss tangents are defined as the ratio of the imaginary part to the real part of the permeability or permittivity as appropriate. This requirement on the dielectric and/or magnetic properties of the material limits the choice of material. This can be a disadvantage when materials with appropriate dielectric and/or magnetic properties have inappropriate physical properties. In addition prior art RAb materials with electric loss are dependent on having thicknesses of the order of, or greater than, a quarter of a wavelength in the material at the frequency of operation. This can also be a disadvantage since prior art RAb materials are often inconveniently thick and bulky in order to achieve the required absorption.

Radar absorbent materials have a range of uses. For instance, at airports where radar is used to monitor the immediate airspace, surfaces which produce strong reflections may be coated with an appropriate RAb material. The radar will operate in practice over a narrow band of frequencies, these being centred on a centre frequency of operation, with a bandwidth of the order of 1%. An appropriate RAb material will therefore be one with a loss of at least 10 dB over the operating bandwidth of the radar system with which it is associated and for which it is designed. This is known as the frequency band of operation of the RAb material.

It is an object of the present invention to provide a frequency selective radar absorbent structure.

The present invention provides a frequency selective radar absorbent structure having a conducting layer and a patterned conducting layer with a central layer sandwiched therebetween, and wherein the central layer has a propagation loss per unit length a, and thickness h, such that, over the frequency band of operation of the structure the product ah lies in the range $0.005 \leq ah \leq 0.1$.

The present invention provides the advantage that it may be constructed with significantly reduced thickness when compared with RAb materials in the prior art. It may therefore be employed in situations where bulky and heavy prior art materils were inappropriate.

The invention may have a control layer such that the product ah lies in the range $0.005 \leq ah \leq 0.05$, or in the range $0.005 \leq ah \leq 0.01$.

The invention may have a central layer with $\mu_r = 1.0$ and thickness h less than or equal to $\lambda/6$, where λ is the wavelength in the central layer of the minimum frequency of operation of the structure.

The invention may be fixed to the surface of a wide range of structures. Such structures may include means of transport including airplanes and ships, and buildings.

In order that it might be more fully understood, embodiments of the invention will now be described, by way of example only, with reference to the accompanying drawings, in which:

Figure 1 schematically illustrates
(a) a section through part of an FSRA structure of the invention,
(b) a plan view indicating the geometry of a slotted array in the conducting layer of the FSRA structure of Figure 1(a), and
(c) a unit cell of the FSRA structure of Figure 1(a);

Figure 2 schematically illustrates one experimental arrangement for measuring the reflected energy from an FSRA structure as a function of frequency;

Figure 3 schematically illustrates one experimental arrangement for measuring the reflected energy in the monostatic direction from an FSRA structure as a function of aspect angle;

Figure 4 graphically illustrates for various angles of incidence the measured power reflection coefficient in the specular direction, as a function of frequency, using the experimental arrangement of Figure 2 and the FSRA structure of Figure 1;

Figure 5 graphically illustrates the predicted power reflection coefficient at various angles of incidence and polarisations in the specular direction as a function of frequency;

Figure 6 graphically illustrates energy absorbed, by the FSRA structure of Figure 1, at 13.0 GHz as a function of incidence angle, using the experimental arrangement Figure 3;

Figure 7 relates to a second embodiment of an FSRA structure of the invention, and schematically illustrates,

(a) a section through part of the FSRA structure,

(b) the smallest unit cell of the FSRA structure,

(c) a hexagonal unit of the FSRA structure, composed of several unit cells, and

(d) a single contiguous element of the hexagonal unit of Figure 7(c);

Figure 8 graphically illustrates the measured energy absorbed at 5° angle of incidence in the specular direction as a function of frequency, using the experimental arrangement of Figure 2, with the FSRA structure of Figure 7;

Figure 9 graphically illustrates the measured energy absorbed at 10.25 GHz as a function of incidence angle, using the experimental arrangement of Figure 3, of the FSRA structure of Figure 7;

Figures 10 to 13 schematically illustrate unit cells of further embodiments of FSRA structures of the invention; and

Figures 14 to 17 graphically illustrate predictions of energy absorbed as a function of frequency at various angles of incidence polarisation for the embodiments of FSRA structure of Figures 10 to 13 respectively.

Referring to Figure 1, three aspects of an FSRA structure 10 of the invention are illustrated schematically. Figure 1(a) shows a section

through part of the FSRA structure 10 indicating its layer structure. Figure 1(b) is a plan view of a layer of the FSRA structure 10 indicating slotted construction. Figure 1(c) shows a unit cell 11 of the FSRA structure 10.

The FSRA structure 10 includes a conducting layer 12, a central layer 14 and a patterned conducting layer 16. The layers 12 to 16 are successively disposed. The thickness of the conducting layer 12 is not critical, and is determined by conventional design considerations. The central layer 14 is of thickness h. The patterned conducting layer 16 is of thickness g and has a periodic pattern, or array, of slots such as 18 extending through it. The periodic pattern of slots can be considered as being built up of unit cells 11, as illustrated in Figure 1(c). The slots 18 are of length ΔX and width ΔY. The unit cells 11 are of length d_x and width d_y with an internal skew angle α between a first side of length d_x and a second side of length $d_y/\sin \alpha$.

For the purposes of this specification, a slot is to be construed as a region of arbitrary shape where there is no conductor or resistive material and which occupies less than 50% of the unit cell area $d_x d_y$.

The patterned conducting layer 16 is of copper of thickness g = 0.034 mm. The central layer 14 is an epoxy glass fibre board with a thickness h = 1.59 mm, and the complex permeability, μ_r, and complex permittivity, ε_r, estimated to be

$$\mu_r = 1.0$$

$$\varepsilon_r = 4.0\ (1 - j \tan \delta_e)$$

where the dielectric loss tangent, $\tan \delta_e$, has the value 0.027. The rectangular slots 18 have dimensions ΔX = 15.0 mm and ΔY = 1.0 mm. The unit cell dimensions are given by d_x = 17.5 mm, d_y = 7.5 mm and α = 41°.

In order to demonstrate the absorbent properties of the FSRA structure 10, a variety of experiments and calculations were carried out. These are now briefly described, and the results obtained discussed.

Referring now to Figure 2, an experimental arrangement 40 for the measurement of specularly reflected energy is illustrated schematically. The arrangement 40 is a conventional Arch system. It includes a synthesised signal source 42, frequency converter 44 and network analyser 46, all controlled by a computer 48 via an IEEE interface bus 50. A transmitting antenna 52 and a receiving antenna 54 are positioned within an arch shaped chamber 56. The chamber 56 has radar absorbent material 58 attached to its internal surfaces 59 to reduce reflections from the surfaces 59. A sample 60 of the FSRA structure under test is located within the chamber 56 and supported by an expanded polystyrene column (not shown). The sample 60 is located such that radiation transmitted from antenna 52, indicated by chain line 62, is incident on the sample 60 at an angle of θ to the normal, indicated by dotted line 64. Specularly reflected radiation, indicated by chain line 66, is reflected at an angle θ to the normal and is incident on the receiving antenna 54. Sample 60 to antenna 52, 54 range is 0.6m.

The measurement procedure employed with the arrangement 40 is as follows. At each angle θ, three measurements M_1, M_2, M_3 of complex received voltage are made. M_1, relates to the sample 60 being located in the chamber 56 as described above. M_2 relates to a flat metal sheet of like dimensions replacing the sample 60. M_3 relates to the chamber 56 empty, ie no sample 60 and no metal plate. The reflectivity of the sample is then calculated using the following equation:

$$\text{reflectivity} = 20\log_{10}\left|\frac{(M_1 - M_3)}{(M_2 - M_3)}\right| \qquad \text{Eq (1)}$$

Referring now to Figure 3, an experimental arrangement 80 for the measurement of monostatic backscatter, or Radar Cross Section, from a sample of a FSRA structure, is illustrated schematically. The arrangement 80 includes a synthesised signal source 82, an amplifier 84, a frequency

converter 86, a network analyser 88, a digital voltmeter 90 and a position drive 92 all controlled via a computer 94 via an IEEE interface bus 96. The signal source 82 supplies a signal, via the amplifier 84, to an antenna 98. The antenna 98 is positioned such that the signals are transmitted into an anechoic chamber 100. A turntable 102 is located with the chamber 100 and is controlled by the position driver 92. A sample 104 of the FSRA structure under test is positioned on the turntable 102, supported on an expanded polystyrene column (not shown). The antenna 98 to sample 104 distance is 3m.

The measurement procedure employed with the arrangement 80 is a continuous wave vector background subtraction technique. At each angle of incidence two measurements of complex received voltage are made. Firstly with an empty chamber 100 and secondly with a sample 104 present. The sample return, or backscatter, at each angle of incidence is then obtained by subtracting the two measurements.

Referring now to Figure 4, results of measurements made on the FSRA structure 10 with the experimental arrangement 40, illustrated in Figure 2, are given graphically. There are shown graphs (a) to (g) inclusive, in each of which the reflection loss in dBs (on the y-axis) is given as a function of frequency of incident radiation in GHz (on the x-axis). Graphs (a) to (d) inclusive show TM polarisation at angles of incidence of θ = 5°, 10°, 15° and 30° respectively. TM polarisation is defined as when the incident magnetic field vector is transverse to the direction of incidence and the normal to the structure aligned so as to be parallel to the slots 18 of the structure. Graphs (e) to (g) inclusive show TE polarisation at angles of incidence of θ = 10°, 15° and 30° respectively. TE polarisation is defined as when the incident electric field vector is transverse to the direction of incidence and the normal to the structure, aligned so as to be perpendicular to the slots 18 of the structure.

Troughs in the reflection loss indicate absorption by the sample 60 at the respective frequencies. Thus it can be seen from Figure 4 that significant absorption occurs, at each angle of incidence, for a small

range of incident frequencies. Figures 4(a), (b) and (c) show two troughs each; 120 and 122, 124 and 126, and 128 and 130 respectively. Figure 4(d) shows one trough 132. Figures 4(e), (f) and (g) show two troughs each; 134 and 136, 138 and 140, and 142 and 144 respectively. This demonstrates that the FSRA structure 10 of the invention provides frequency selective absorption.

Referring now also to Figure 5, computer predictions corresponding to the experimental results of Figure 4 are illustrated graphically. The predictions are based on a FSRA structure model which is infinite with no edges. The model is in place of the finite sample 60, as is common in such computations. It is further assumed that the conductor 16, is perfect with zero thickness ($g = 0$). Other aspects of the FSRA structure 10 were modelled as closely as possible with the exception of the substrate thickness h, which was set at 1.570 mm in place of 1.590 mm. These are within the range of tolerance for the nominal substrate thickness of 1/16 of an inch. Predictions were made every 0.1 GHz, and these predictions were joined using tight fitting curves. It should be noted that the axes of the graphs of Figure 5 are identical to those of Figure 4, including the ranges covered. As for Figure 4, graphs (a) to (d) inclusive show TM polarisation at angles of incidence $\theta = 5°$, 10°, 15° and 30° respectively, whilst graphs (e) to (f) inclusive show TE polarisation at angles of incidence $\theta = 10°$, 15° and 30° respectively.

The graphs of Figure 5 all show troughs in the reflection loss at all angles of incidence. Figures 5(a), (b) and (c) show two troughs each; 150 and 152, 154 and 156, and 158 and 160 respectively. Figure 5 (d) shows one trough 162. Figures 5(e), (f) and (g) show two troughs each; 164 and 166, 168 and 170, and 172 and 174 respectively. When comparing graphs (a) to (g) of Figure 5 with the respective graphs of Figure 4 it can be seen that the general pattern of the predictions is the same as the pattern of the experimental results. However, the majority of the troughs 150 to 174 are shifted up in frequency when compared with the troughs 120 to 144. Such an offset between the two sets of data may well be accounted for by

the differences between a finite sample and an infinite structure, or by an error in the estimated value of ε_r.

Referring now to Figure 6, experimental results obtained using the arrangement 80, of Figure 3, are illustrated graphically. The relative radar cross sections of the FSRA structure 10 and a similar sized metal plate are shown in curves 190 and 192 respectively, for angles of incidence between ± 40° and TE polarisation. A reduction of 13 dB in the normal incidence (0°) backscatter, when comparing the FSRA structure 10 with the metal sheet, is demonstrated. The FSRA structure 10 of the invention consequently provides a potentially important reduction in radar cross-section.

Referring now to Figure 7, an alternative embodiment 200 of an FSRA structure of the invention is illustrated schematically. Figure 7(a) shows a section through part of the FSRA structure 200 indicating its layer structure. Figure 7(b) illustrates a unit cell 202 of the FSRA structure 200. Figure 7(c) illustrates a hexagonal unit 204 composed of several unit cells 202. Figure 7(d) illustrates a single contiguous conducting element 206.

The FSRA structure 200 includes a conducting layer 212, a central layer 214 and a patterned conducting layer 216. The thickness of the conducting layer 212 is not critical. The central layer 214 is of thickness h. The patterned conducting layer 216 is of thickness g and has a periodic pattern, or array, of elements such as 206. The periodic pattern of elements can also be considered as being built up of unit cells such as 202. The hexagonal unit 204 shows more clearly how the periodic pattern is composed of interlocking, but not connected, elements 206. The unit cells 202 are of length d_x and width d_y with internal skew angle α, between a first side of length d_x and a second side of length $d_y/\sin\alpha$.

In this embodiment the patterned conducting layer 16 is of copper of thickness g = 0.0012 mm. The central layer 14 is as used in the FSRA

structure 10. The unit cell dimensions are given by d_x = 15.00 mm, $d_y = 15\sqrt{3}/2$ mm ≈ 12.00 mm and $\alpha = 60°$.

In order to demonstrate the radar absorbent properties of the FSRA structure 200, experiments were carried out as for the FSRA structure 10.

Referring now to Figure 8 the results of measurements made on a sample of the FSRA structure 200 with the experimental arrangement 40 of Figure 2, are illustrated graphically. The angle of incidence is 5°, and at this angle the results are independent of polarisation to within measurement tolerances. The reflection loss in dB is given as a function of frequency between 8 and 18 GHz. A trough 220 indicates a reduction in reflection of 18.5 dB at 10.25 GHz.

Referring now to Figure 9, results of measurements made on a sample of the FSRA structure 200 using the experimental arrangement 80 of Figure 3 are illustrated graphically. The relative radar cross section in dB's of the FSRA structure 200 and a similar sized metal plate are given by curves 230 and 232 respectively, for angles of incidence between ± 40° and TE polarisation. A reduction of 20 dB is demonstrated at normal incidence (0°).

The results of Figures 8 and 9 indicate that the FSRA structure 200 exhibits significant frequency selective absorption, and a significant reduction in radar cross section.

Referring now to Figures 10, 11, 12 and 13, unit cells of further embodiments of FSRA structures of the invention are illustrated schematically, shaded areas being conductor (copper). All four embodiments shown in respective ones of these Figures have a layered structure (not shown) similar to that of the FSRA structure 10, with g = 0.0 mm and h = 1.59 mm. Figure 10 shows a unit cell 240 including a slot 242, with dimensions ΔX by ΔY, in a patterned conducting layer 244. Figure 11 shows a unit cell 250 including an element 252, with dimenensions ΔX by ΔY. Elements such as the element 252 form a patterned

conducting layer 254. Figure 12 shows a unit cell 260 including a slot 262, with dimensions ΔX by ΔY, in a patterned conducting layer 264. Figure 13 shows a unit cell 270 including a conducting element 272 with dimensions ΔX by ΔY. All the unit cells 240, 250, 260 and 270 have dimensions d_x, d_y and α all have the same values as for the FSRA structure 10. The central layers of the embodiments of Figures 10 and 11 have complex permeability and permittivity given by

$$\mu_r = 2.0\ (1 - j\tan\delta_m)$$
$$\tan\delta_m = 0.432$$
$$\varepsilon_r = 1.0$$

The central layers of the embodiments of Figures 12 and 13 have complex permittivity and permeability given by

$$\mu_r = 1.0$$
$$\varepsilon_r = 2.0\ (1 - j\tan\delta_e)$$
$$\tan\delta_e = 0.216$$

Having shown for the FSRA structure 10 that the computer predictions agreed closely with the experimental results, computer calculations were carried out to demonstrate the absorbent properties of the FSRA structures of Figures 10 to 13.

Referring now to Figures 14, 15, 16 and 17, computer predictions of reflection, in the specular direction, from the embodiments of FSRA structure of Figures 10, 11, 12 and 13 respectively, are illustrated graphically. The reflection in dB is given as a function of frequency for TE and TM incident polarisations at the following angles of incidence; normal, 15°, 30°, 45° and 60°. The FSRA structures modelled were infinite with no edges. The results show clearly that significant reduction in reflection can be achieved by an FSRA structure of the invention at certain frequencies of incident radiation.

Radar absorbent materials in the prior art are designed specifically for each application. This is also the case for FSRA structures of the invention. As Figures 4,5,6,8,9 and 14 to 17 show FSRA structures may be designed to operate, or absorb, over a particular frequency range, for particular angles of incidence and for a particular polarisation. The phrase frequency of operation is taken to include, not only the frequency, but also the angle of incidence and polarisation, at which a FSRA structure is designed to operate. If a FSRA structure operates over a waveband then there will be range of frequencies of operation.

For instance a surveillance radar at an airport will operate over a narrow waveband, centred at a nominal frequency of operation with a bandwidth of the order of 1%. Buildings in and around the airport may be coated with appropriately designed FSRA structures in order to prevent strong reflections swamping useful signals. Such FSRA structures will be designed to absorb the waveband of operation of the radar at appropriate angles of incidence and polarisation. That is it will have a range of frequencies of operation covering at least the waveband of the radar and preferably centred at the nominal frequency of operation of the radar.

A reduction in reflection such as that illustrated in Figures 4 to 6 and 8 and 9 indicates that energy is being absorbed. A dominant absorption mechanism, responsible for the absorption illustrated in Figures 4 to 6 and 8 and 9, may be shown to be due to the excitation of surface waves within the structure of the FSRA structure concerned. In particular, the total power loss per unit area in an FSRA structure consisting of a conducting pattern above a homogeneous dielectric/magnetic substrate backed by a conductor may be shown to be given by the expression,

$$P_t = \sum_{pqr} |T_{pqr}|^2 W_{pqr}^{(t)} \quad \text{for } -\infty \le p \le \infty, -\infty \le q \le \infty, \; r = 1,2$$

where $|T_{pqr}|^2 W_{pqr}^{(t)}$ is the power loss per unit area in the p,q,r^{th} surface mode (except for p=q=0 which corresponds to the dominant ray mode which is not a surface wave mode). $W_{pqr}^{(t)}$ is given by,

$$W_{pq1}^{(t)} = \Re\left\{ \frac{1}{2\eta_o k_o \mu_r^*} Y_{pq}^* \left(1 - |f_{pq}^-(2d)|^2 + f_{pq}^{-*}(2d) - f_{pq}^-(2d)\right)\right\}$$

and

$$W_{pq2}^{(t)} = \Re\left\{ \frac{1}{2\eta_o k_o \mu_r^*} \left(Y_{pq}^* + t_{pq}^2/Y_{pq}^*\right)\left(1 - |f_{pq}^-(2d)|^2 + f_{pq}^{-*}(2d) - f_{pq}^-(2d)\right)\right\}$$

where η_o is the impedance of free space, k_o is the free space wave number, '*' represents the complex conjugate, μ_r is the complex permeability of the central layer, $\Re$ represents the 'real part of', d is the central layer thickness and Y_{pq}, t_{pq} and f_{pq}^- are given by

$$Y_{pq} = \left(\varepsilon_r \mu_r k_o^2 - t_{pq}^2\right)^{1/2}, \quad \Im(Y_{pq}) \le 0$$

$$t_{pq}^2 = u_{pq}^2 + v_{pq}^2$$

$$u_{pq} = k_o \sin\theta_o \cos\phi_o + 2\pi p/d_x$$

$$v_{pq} = k_o \sin\theta_o \sin\phi_o + 2\pi q/d_y - 2\pi p/(d_x \tan\alpha)$$

$$f_{pq}^-(2d) = \exp(-jY_{pq}2d)$$

where d_x,d_y and α are the unit cell dimensions, ε_r is the complex permittivity of the central layer and θ_o and ϕ_o are the angles of incidence (with respect to the normal, and x-axis respectively) of the incident wave in free space. $\Im$ represents the "imaginary part of".

The transmission coefficient T_{pqr} is dependent on the FSRA structure geometry and is not in general known a-priori. However, if the field distribution, $\underline{F}(\underline{x})$ is known on the aperture (eg by using the method of moments, or by using an approximate distribution for simple geometries) then T_{pqr} may be determined using,

$$T_{pqr} = \frac{2A_{oos}\xi^{(1)}_{oos}L^{*}_{oos}L_{pqr}}{(1 - f^{-}_{pq}(2d))\sum_{mnt} G_{mnt}|L_{mnt}|^2}$$

where A_{oos} is the amplitude of the incident field in polarisation state s = 1,2 and

$$G_{pqr} = \xi^{(1)}_{pqr} + \frac{(1 + f^{-}_{pq}(2d))}{(1 - f^{-}_{pq}(2d))}\xi^{(2)}_{pqr}$$

$$\xi^{(1)}_{pqr} = \begin{cases} \sqrt{(k_o^2 - t_{pq}^2)}/(k_o\eta_o), r = 1 \\ k_o/(\eta_o\sqrt{(k_o^2 - t_{pq}^2)}), r = 2 \end{cases} \quad \text{non-positive imaginary part}$$

$$\xi^{(2)}_{pqr} = \begin{cases} \gamma_{pq}/(\mu_r k_o\eta_o), r = 1 \\ \varepsilon_r k_o/(\gamma_{pq}\eta_o), r = 2 \end{cases} \quad \text{non-positive imaginary part}$$

$$L_{pqr} = \int_{\text{aperture}} \underline{F}(\underline{x}).\underline{\Phi}^{*}_{pqr}(\underline{x})\,dx$$

and

$$\underline{\Phi}_{pqr}(\underline{x}) = \begin{cases} (d_x d_y)^{-0.5}\left(\frac{v_{pq}}{t_{pq}}\hat{\underline{x}} - \frac{u_{pq}}{t_{pq}}\hat{\underline{y}}\right)\exp(-j[u_{pq}x + v_{pq}y]), r = 1 \\ (d_x d_y)^{-0.5}\left(\frac{u_{pq}}{t_{pq}}\hat{\underline{x}} + \frac{v_{pq}}{t_{pq}}\hat{\underline{y}}\right)\exp(-j[u_{pq}x + v_{pq}y]), r = 2 \end{cases}.$$

The surface waves, described in the expression for P_t, propagate in the substrate in a direction parallel to the surface adjacent to the slotted or patterned conducting layer and thereby allow energy to be absorbed in this direction. This contrasts with prior art radar absorbent (RAb) material in which surface wave modes are not excited and energy can thereby only be absorbed in the direction of the principal ray path within the medium. This limitation of the prior art means that it requires a substrate which must be substantially thicker than that of an FSRA structure of the invention in order to provide sufficient path length for energy to be absorbed.

This may be quantified as follows. Propagation loss per unit length, a, is defined by

$$\gamma = a + jb$$

where

$$\gamma = j\omega\sqrt{\varepsilon\mu},$$

j being the square root of minus one, ω the angular frequency of the incident radiation, and ε and μ the permeability and permittivity of the medium respectively. In prior art RAb material the wave in the medium takes the form

$$\underline{E} = \underline{E}_o e^{(j\omega t - \gamma z)}$$

where t is time and z is distance normal to the surface of the RAb material.

If the thickness of the medium is taken to be h, then for a reflection loss greater than or equal to 10 dB, over the range of frequencies of operation, prior art RAb material exhibits

$$ah \geq 0.3$$

for FSRA structure of the invention, for a reflection loss greater than or equal to 10 dB, over the range of frequencies of operation then ah is within the range

$$0.005 \leq ah \leq 0.1$$

For instance the FSRA structure 10 of Figure 1 has a value of ah of 0.009, over its range of frequencies of operation.

In prior art RAb materials with no magnetic loss, and thus only electric loss, the substrate thickness h is required to be greater than or equal to $\lambda/4$, where λ is the wavelength of radiation within the central layer for the minimum radar frequency for which the RAb material is designed, for a reflection loss greater than or equal to 10 dB. Such limitations are discussed by E F Knott in "The Thickness Criterion for Single-Layer Radar Absorbents", IEEE Trans A P, Vol AP-27, No 5, Sept 1979, pp698-701. For FSRA structures of the invention this requirement is significantly relaxed, and reflection losses of greater than or equal to 10 dB at the frequency of operation may be achieved with h less than $\lambda/6$. This is a surprisingly low value of h and is advantageous in that it reduces bulk and may reduce cost. Such losses are achievable provided the thickness h does not become so small that the excitation of surface waves is prevented.

The use of the term 'Radar' in the description of this invention reflects the principle use of the invention. However, the invention is not limited to use as an absorber of electromagnetic waves with frequencies in the range traditionally described as radar frequencies. When appropriately designed, embodiments of the invention may be used in other regions of the electromagnetic spectrum, for instance in the infra red.

Various patterned conducting layers 16, 216, 244, 254, 264 and 274 are incorporated in the embodiments of FSRA structure described above. In general a patterned conducting layer is a layer of conducting material with a periodic pattern of slots cut through it, or a layer including a

periodic pattern of elements of a conducting material. A patterned conducting layer may also include both slots and elements.

CLAIMS

1 A frequency selective radar absorbent structure having a conducting layer and a patterned conducting layer with a central layer sandwiched therebetween, and wherein the central layer has a propagation loss per unit length a, and thickness h, such that, over the frequency band of operation of the structure the product ah lies in the range $0.005 \leq ah \leq 0.1$.

2 A frequency selective radar absorbent structure according to Claim 1 wherein the product ah lies in the range $0.005 \leq ah \leq 0.05$.

3 A frequency selective radar absorbent structure according to Claim 2 wherein the product ah lies in the range $0.005 \leq ah \leq 0.001$.

4 A frequency selective radar absorbent structure according to Claim 1 wherein, i) the central layer has $\mu_r = 1.0$, and ii) the central layer thickness h is less than or equal to $\lambda/6$ where λ is the wavelength in the central layer of the minimum frequency of operation of the structure.

5 A frequency selective radar absorbent structure according to any preceding claim fixed to the surface of a means of transport.

6 A frequency selective radar absorbent structure according to any one of claims 1 to 4 fixed to the surface of a building.

Amendments to the claims have been filed as follows

1 A frequency selective radiation absorbent structure having a conducting layer and a patterned conducting layer with a central layer sandwiched therebetween, wherein the structure is arranged for absorption of electromagnetic radiation by surface waves.

2 A frequency selective radiation absorbent structure according to Claim 1 wherein the central layer has a propagation loss per unit length a, and thickness h, such that, over the frequency band of operation of the structure the product ah lies in the range $0.005 \leq ah \leq 0.1$.

3 A frequency selective radiation absorbent structure according to Claim 2 wherein the product ah lies in the range $0.005 \leq ah \leq 0.05$.

4 A frequency selective radiation absorbent structure according to Claim 3 wherein the product ah lies in the range $0.005 \leq ah \leq 0.01$.

5 A frequency selective radiation absorbent structure according to Claim 2 wherein, i) the central layer has $\mu_r = 1.0$, and ii) the central layer thickness h is less than or equal to $\lambda/6$ where λ is the wavelength in the central layer of the minimum frequency of operation of the structure.

6 A frequency selective radiation absorbent structure according to any preceding claim fixed to the surface of a means of transport.

7 A frequency selective radiation absorbent structure according to any one of claims 1 to 5 fixed to the surface of a building.

Patents Act 1977

Examiner's report to the Comptroller under Section 17 (The Search Report)

Relevant Technical fields

(i) UK Cl (Edition K) H1Q (QEJ, QEC, QEX, QKJ)

(ii) Int Cl (Edition 5) H01Q

Databases (see over)

(i) UK Patent Office

(ii) -

Search Examiner

MR J BETTS

Date of Search

14 SEPTEMBER 1992

Documents considered relevant following a search in respect of claims 1 to 6

Category (see over)	Identity of document and relevant passages	Relevant to claim(s)
E,X	GB 2251338A (Sec State Defence) see page 3	1-4
X	EP 0015804A (Thomson-CSF) see Figure 2c	1-4
X	US 3887920A (Wright) Whole doc	1-4